

**Abstracts of the Papers Published by the
Staff Members of the Institute from
July, 1971 to June, 1972**

Nuclear Chemistry

Elastic Scattering of 100— and 200-keV Positrons by Selenium and Bismuth. T. Kobayashi and S. Shimizu. *Bull. Inst. Chem. Res., Kyoto Univ.*, **50**, 488 (1972).—The differential cross sections for elastic scattering of positrons in ^{34}Se and ^{83}Bi targets were measured at 30° , 40° , 60° and 85° for energies of 100 and 200 keV. Positron beams of these energies were obtained by the use of a sector-type double-focusing β -ray spectrometer mounted with a ^{22}Na source. Scattered positrons were measured by semiconductor (silicon) detectors in a scattering chamber. The experimental results were compared with the theoretical values calculated by the Mott phase-shift method. Though the experimental cross sections were, on the whole, in agreement with the theoretical values, the experimental cross sections tend to be lower than the theoretical ones, especially in the case of 100-keV positron scattering in Bi targets. This phenomenon was considered to be due to the effect of local distortion of the electron cloud by the incident particle.

A Proportional Counter for Mössbauer Spectroscopy by Scattered Electrons. M. Takabuchi, Y. Isozumi, and R. Katano. *Bull. Inst. Chem. Res., Kyoto Univ.*, **51**, 13 (1973).—A proportional counter with a very small sensitive volume ($250\text{ mm}^2 \times 3\text{ mm}$) has been constructed for Mössbauer spectroscopy by scattered electrons. More than 20% effect with a 100% baseline has been obtained for an unenriched sample of Type 310 stainless steel with a helium-10% methane mixture flowing through the counter. Some features of the counter are described.

Mössbauer Effect in SnI_4 . R. Katano and T. Mukoyama. *Bull. Inst. Chem. Res., Kyoto Univ.*, **51**, 19 (1973).—Mössbauer measurements of the 23.8-keV transition in ^{119}Sn and of the 57.6-keV transition in ^{124}I have been carried out in order to investigate the chemical bond in SnI_4 . The isomer shifts for Sn and for I have been obtained. These data combined with the iodine NQR data of the quadrupole splitting have been used to interpretate the bond structure. The Sn-I bond in SnI_4 contains about 23% π -character, and 5% s -hybridization is presented in the iodine σ -orbital. These results are in good agreement with the previous interpretation of the Mössbauer experiments for ^{119}Sn and ^{129}I . The effective charge on the iodine atom is $-0.022e$ and that on the tin atom is $+0.088e$.

Two-Photon Decay of the 1.76-MeV O^+ State of ^{90}Zn . Y. Nakayama. *Phys. Rev. C*, **7**, 322 (1973).—Measurements of the probability and the energy distribution for the two-photon decay from the 1.76-MeV O^+ first excited state to the

O^+ ground state of ^{90}Zr have been performed using a sum-coincidence technique with an antidetector and large lead shields. This improved experimental technique made it possible to eliminate unfavorable coincident events which would disturb true events from the two-photon process. The ratio of two-photon decay to the sum of internal-pair decay and internal-conversion decay, $T_{\gamma\gamma}/T_{\alpha+\beta}$, has been found to be $(5.1 \pm 2.5) \times 10^{-4}$. This value is larger than the upper limits reported recently by other workers, and not consistent with any values calculated based on existing theories. The energy spectrum of one of two photons has also been observed. This spectrum suggests reasonably that two-photon decay takes place as an $(E1, E1)$ transition via giant-dipole-resonance states. A discussion of the theoretical significance of this study is given.

100 and 200 keV Positron Scattering by Atomic Nuclei. T. Kobayashi and S. Shimizu. *J. Phys. B: Atom. Molec. Phys.*, **5**, L211 (1972).—The differential cross sections for elastic scattering of positrons by Se and Bi were measured at 30° , 40° , 60° and 85° for energies of 100 and 200 keV, and compared with the Mott theory. Though the experimental results were, on the whole, in agreement with the theory, the measured cross sections tend to be a little lower than the theoretical ones.

Recent Developments of the Study on the K-Shell Internal Ionization in Beta Decay. S. Shimizu. *Proc. International Conf. on Inner Shell Ionization Phenomena and Future Applications, April 17–22, 1972, CONF-720404*, **3**, 2050 (1973).—This paper reviews recent experiments to study the phenomenon by measuring the energy-dependent ionization probability $P_K(E_\beta^\circ)$ as a function of E_β° , where the parameter E_β° is defined as a sum of energies of β particle, E_β , and emitted K electron, E_K , plus K -shell binding energy of the daughter atom, B_K . The one-step theory of the electron shakeoff developed by Stephas and Crasemann has been improved by using the energy-dependent antisymmetrization factor $E(E_\beta, E_K)$ and the exact relativistic hydrogenic atomic matrix element. It has been found that the experimental $P_K(E_\beta^\circ)$ deviates considerably from that predicted by this improved theory, suggesting that the direct collision process may play an important role in the low energy region of E_β° . As to the total ionization probability the improved theory can give the values in fairly good agreement with the measured values.

Nuclear Phenomena Involving Shell Electrons. S. Shimizu. *Japanese Scientific Monthly (Gakujutsu Geppo)*, **25**, 562 (1972), in Japanese.—The sketchy review is presented on the experimental works concerning the nuclear phenomena involving shell electrons, which have been and/or are being performed in our Laboratory for the past several years, as follows: I) Positron annihilation by K -shell electrons—single-quantum annihilation, radiationless annihilation, nuclear excitation by positron annihilation; II) External effects on the decay constant of radioactive nuclei - by chemical bonding for ^{235m}U , by high pressure for ^{99m}Tc , and by internal electric field for ^{99m}Tc in $BaTiO_3$; III) K -shell internal ionization accompanying beta decay.

The $D(p, 2p)n$ Reaction at 3.8 to 5.0 MeV. S. Matsuki, K. Ogino, E. Takasaki, M. Yasue, K. Tsuji, N. Izutsu, and S. Yamashita. *Proceedings of the International Con-*

ference on Few Particle Problems in the Nuclear Interaction (Los Angeles, August 28-September 1, 1972). 535 (1972).—A deuterated polyethylene target was bombarded with protons from 3.8 to 5.0 MeV. Coincidence counting between two protons were done by using two silicon detectors, time to amplitude converter and a two dimensional pulse height analyzer. Energy spectra of coincided protons were obtained at 7 incident energy steps, and also the excitation function of this reaction. The interference between two pairs of proton-neutron were observed at low incident energy but the evidence of singlet deuterons was not obtained. From the analysis of the excitation function, it was concluded that no excited state of ^3He exist in the energy range observed.

Structure of ^{10}B Formed by the Reaction $^9\text{Be}+p$. M. Yasue, T. Ohsawa, N. Fujiwara, S. Kakigi, D. C. Nguyen, and S. Yamashita. *Proceedings of the International Conference on Few Particle Problems in the Nuclear Interaction (Los Angeles, August 28-September 1, 1972)*, 1009 (1972).—Levels of ^{10}B near 10 MeV excitation were studied with the reaction $^9\text{Be} + p$ in the energy range of protons from 4 to 6 MeV. The effect of the final state interactions between n and $^8\text{Be}(g'nd)$ were studied for the reaction $^9\text{Be}(p, p_1)^9\text{Be}$ (1.67 MeV). The energy spectra of p_1 were analyzed to give the scattering length between n and ^8Be and then it is concluded that the structure of $^{10}\text{B}(11.2 \text{ MeV})$ state is [$^8\text{Be}(0^+) + n$ (s-state) + p (d-state)].

Three Body Break-Up of ^{12}C by 52 MeV Protons. S. Yamashita, K. Fukunaga, S. Kakigi, N. Fujiwara, T. Ohsawa, K. Takimoto, K. Ogino, I. Yamane, M. Yasue, N. Izutsu, and D. C. Nguyen. *Proceedings of the International Conference on Few Particle Problems in the Nuclear Interaction (Los Angeles, August 28-September 1, 1972)*, 1006 (1972).—Protons and alpha particles emitted in coincidence from the $^{12}\text{C}(p, p\alpha)$ reaction were detected. Summed energy spectrum of protons and alpha particles show peaks corresponding to the states of ^{12}C of 19.3, 21.6, 25.8 and 30 MeV excitation, and indicate these alpha particles are emitted when the excited ^{12}C nucleus breaks into three alpha particles. The angular correlation functions between those protons and alpha particles which correspond to the definite excited state of ^{12}C indicate that the 21.6 MeV state of ^{12}C could have a structure different from other excited states.

Excited States of ^{10}B near 10 MeV Studied by Proton Induced Reactions on ^9Be . M. Yasue, T. Ohsawa, N. Fujiwara, S. Kakigi, D. C. Nguyen, and S. Yamashita. *J. Phys. Soc. Japan*, **33**, 265 (1972).—Excitation functions for the $^9\text{Be}(p, p)^9\text{Be}$ reaction were measured in the energy range of protons from 4 to 6 MeV, using a Tandem Van de Graaff accelerator of Kyoto University. The 10.8 MeV excited state of ^{10}B was observed in the $^9\text{Be}(p, p_2)^9\text{Be}(2.43)$ reaction. The width of this excited state was estimated to be 300 keV. In the excitation function for the $^9\text{Be}(p, p_1)^9\text{Be}$ (1.67) reaction, an enhancement was observed around $E_p=5.1$ MeV. Assuming this enhancement to be due to the compound state of ^{10}B nucleus, the excitation energy of this state is 11.2 MeV. In the $^9\text{Be}(p, p_0)^9\text{Be}(g'nd)$ reaction, a broad enhancement was observed around $E_p=4.5$ MeV.

Analytical Chemistry

Separation by Coprecipitation. T. Shigematsu. *Japan Analyst*, **22**, 618 (1973), in Japanese.—Review.

Fluorometric Determination of Selenium in Sea-Water. K. Hiraki, O. Yoshii, H. Hirayama, Y. Nishikawa, and T. Shigematsu. *Japan Analyst*, **22**, 712 (1973), in Japanese.—2,3-Diaminonaphthalene reacts with selenium(IV) to form a complex with greenish yellow fluorescence, which are extracted into organic solvents, such as cyclohexane, toluence *etc.*, and was used as a sensitive reagent for the fluorometric determination of selenium. The authors have studied on the fluorometry of selenium with the reagent, and the method was adopted for analysis of selenium in sea-water.

Fifty milliliters of conc. HCl and 20 mg of Fe^{3+} as FeCl_3 solution were added to 5 l of sample sea-water, and pH of the solution was adjusted to 5.5 with ammonia. After a few hours 5 mg of Fe^{3+} and ammonia were added to the solution. This procedure was repeated. After being allowed to stand overnight, the precipitate was filtered and washed with water, then dissolved in 5–6 ml of 6 N HCl. Three milliliters of 1 M sodium acetate solution was added to the solution and pH was adjusted to 1 by adding conc. HCl, and the total volume was made up to 30 ml. To remove Fe^{3+} , the solution was poured into an ion-exchange colume [Dowex 50 WX8 (H-form), ϕ : 30 mm, height: 50 mm], and the column was eluted with 0.1 M sodium acetate solution (pH of the solution was adjusted to 1 with hydrochloric acid, flow rate=1.3 ml/min). The selenium, fraction of the eluant was evaporated to 10 ml. Five milliliters of 0.1% 2,3-diaminonaphthalene solution, 0.5 ml of 0.1 M EDTA solution, and 0.5 ml of 0.1 M sodium fluoride solution were added to this solution, and pH of the solution was adjusted to 1 with hydrochloric acid or ammonia. The solution was diluted to 25 ml and heated at 50°C for 20 min. After being cooled to room temperature, the solution was extracted with 10 ml of cyclohexane. The organic layer was separated and dehydrated by centrifugation, and the fluorescence intensity was measured at 520 nm (excitation: 375 nm) against the standard uranine solution (0.0625 $\mu\text{g}/\text{ml}$). In this procedure, the recovery of selenium was about 90%.

Selenium contents in the sea-waters offshore of Misaki (Osaka Pref.), Yuasa and Uragami (Wakayama Pref.) were found to be 0.01–0.07 $\mu\text{g}/\text{l}$. The amounts of dissolved selenium and the particle size distribution of selenium in suspended matter were determined successfully by the present procedure.

Quantitative Treatment of the Distribution Coefficient for Coprecipitation of Metal Oxalates. M. Munakata and S. Toyomasu, and T. Shigematsu. *Anal. Chem.*, **44**, 2057 (1972).—The distribution coefficient, λ , of coprecipitation in binary metal oxalates, calcium-strontium, calcium-rare earth and rare earth-rare earth, is discussed as based on precipitation rate and solubility products. In the calcium-rare earth systems, the coefficients equal the ratio of the apparent rate constants for the precipitation. The distribution coefficient in the calcium-strontium oxalate system was determined by the ratio of the solubility products rather than the

rate constants. Neither the solubility product nor precipitation rate, however, was correlated to the distribution coefficient of the coprecipitation for rare earth-rare earth oxalate systems.

Spectrophotometric Determination of Palladium with Eriochrome Cyanine R. T. Shigematsu, M. Matsui, and K. Uesugi. *Bull. Inst. Chem. Res., Kyoto Univ.*, **50**, 634 (1972).—A new spectrophotometric method for the determination of palladium was studied, using eriochrome cyanine R as a reagent. Palladium reacts very sensitively with eriochrome cyanine R in the presence of tetradecyldimethylbenzylammonium chloride (TDBA) to form a colored complex. The palladium complex in the presence of TDBA gives the higher order complex with its absorption maximum shifted to longer wavelengths. The complex shows maximum absorbance at the pH range from 4.0 to 5.6; Beer's law is obeyed over the range from 0.1 to 1.2 ppm of palladium at 620 nm. The molar absorptivity is 99,000 and the sensitivity is 0.0011 μg of palladium per cm^2 , corresponding $\log I_0/I=0.001$. The mole ratio of palladium and reagent in the complex is estimated to be 1: 3 in the presence of TDBA. Copper (II) and iron (III) interfere with the determination of palladium when sodium fluoride is used as a masking agent. This method is the most sensitive among the methods using some triphenylmethane dyes, which have structures similar to this reagent.

Coprecipitation of Copper with Hydroxyapatite. T. Shigematsu, O. Fujino, and M. Matsui. *Bull. Inst. Chem. Res., Kyoto Univ.*, **50**, 645 (1972).—The distribution behavior of cupric ion between aqueous phase and hydroxyapatite crystal was investigated. The apatite prepared by adding phosphate ion extremely slowly in calcium solution at 80°C, yielded a X-ray diffraction pattern of hydroxyapatite and had a composition that Ca/P molar ratio was 1.67 at pH 7.80. Apparently, the coprecipitation reaction seems to be anomalous, because the apparent distribution coefficient did not have a constant value through the reaction. But when true distribution coefficient was calculated, it was revealed that cupric ion was coprecipitated obeying logarithmic distribution law. Cupric ion seems to be somewhat unstable in the apatite crystal, judging from the influence of copper concentration.

The Solvent Extraction of Zinc Pivaloyltrifluoroacetone Adducts with Monodentate and Bidentate Ligands. K. Ueda, T. Aoki, M. Matsui, and T. Shigematsu. *Bull. Inst. Chem. Res., Kyoto Univ.*, **50**, 653 (1972).—The effect of the monodentate and bidentate neutral ligands acting as a synergist on the extraction of zinc with pivaloyltrifluoroacetone was investigated. TPPO, TOPO and TPAsO were used as neutral monoxide ligands, MBDPO and EBDPO as dioxide ligands, pyridine, picolines and 2,6-lutidine as monodentate N-bases, and α, α' -dipyridyl and bathophenanthroline as bidentate N-bases. Ligands containing oxygen react with zinc chelate to form the adducts of MR_2L type, and the stability constant of the adducts increases in the following order: TPPO < EBDPO < MBDPO < TOPO < TPAsO. The stability of adducts with pyridine bases increases in the order, 2,6-lutidine < α -picoline < pyridine < γ -picoline. A striking synergistic effect was observed in the presence of α, α' -dipyridyl and bathophenanthroline.

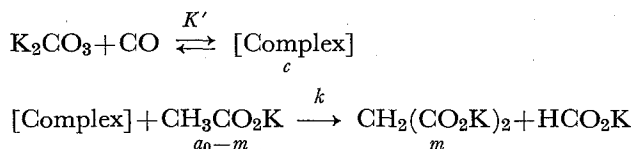
Physical Chemistry

Kinetic Study of Potassium Malonate Synthesis from Potassium Acetate, Carbonate and Carbon Monoxide under Pressure. K. Kudo, N. Sugita, and Y. Takezaki. *Nippon Kagaku Kaishi*, 1082 (1973), in Japanese.—Synthesis of potassium malonate from potassium acetate, carbonate and carbon monoxide has been studied kinetically under pressure in a molten potassium formate solution.

The initial rate of malonate formation is of the first order with respect to carbon monoxide pressure and the mole ratio of acetate/carbonate in the charge.

Potassium carbonate reacted with carbon monoxide under malonate producing conditions to give a complex, which was decomposed in water into potassium formate and bicarbonate. The addition of malonate and formate, the reaction products, into the system had no effect on the malonate formation.

Based on these results following mechanism has been proposed: potassium carbonate reacts first with carbon monoxide to form a complex as an intermediate, with which acetate converts into dipotassium malonate and potassium formate.



The rate equation and equilibrium constant given by

$$V_0' = kK'P_{\text{CO}}(a_0/b_0) \quad \text{and} \quad K' = c/P_{\text{CO}}N,$$

where a_0 : charge acetate (mol), b_0 : charge carbonate (mol), P : CO pressure (kg/cm²), N : total mole, K' : apparent equilibrium constant, expressed the observed kinetic results satisfactorily.

The apparent equilibrium constants of the complex formation and rate constants have been determined at 265, 280 and 300°C to be $K' = 2.125, 3.874$ and 6.801×10^{-4} (kg/cm²)⁻¹, and $k = 3.192, 3.788$ and 4.450×10^{-2} min⁻¹, respectively. The overall activation energy and apparent heat of complex formation are found to be 26.1 kcal and 19.6 kcal, respectively.

Studies of Built-up Films by Means of the Polarized Infrared ATR Spectrum. II. Mixed Films of Stearic Acid and Barium Stearate. T. Takenaka, K. Nogami, and H. Gotoh. *J. Colloid Interface Sci.*, 40, 409 (1972).—Polarized infrared attenuated total reflection studies have been made of mixed multilayers of stearic acid and barium stearate built up on a germanium plate by the Blodgett technique. Infrared transmission spectra of the built-up films have also been recorded by using polarized radiation. It is concluded that the films are made of an assembly of crystallites of the triclinic system, where all the *trans*-zigzag planes of the hydrocarbon chains are parallel to one another. The orientation of the hydrocarbon chains in the germanium-sample interface is found to be independent of the dipping direction of the plate during the process of monolayer transfer, while largely dependent upon the polishing direction of the plate in its cleaning procedure. The angle between

the plane of the hydrocarbon chains and the polishing direction is estimated to be *ca.* 40° with the aid of reflectivities of the polarized radiations at 2920 and 2850 cm⁻¹ and the dichroic ratio in the polarized transmission spectra.

Furthermore, from the penetration depth of the totally reflected radiation and changes in reflectivity with the number of layers, the film thickness per layer is found to be *ca.* 24.3 Å, being in good agreement with the half of the long spacing, 49.06 Å, of the mixed films determined by X-ray diffraction studies.

Studies of Built-up Films by Mean of the Polarized Infrared ATR Spectrum. III. Elaidic Acid Films. T. Takenaka and K. Nogami. *Bull. Chem. Soc. Japan*, **45**, 2367 (1972).—Attenuated total reflection studies with polarized infrared radiation have been made of multilayers of elaidic acid built up on a germanium plate by the Blodgett technique. It is concluded that the built-up films prepared from the tap-water substrate are made of calcium elaidat monohydrate. From the intensity changes in the regularly-spaced peaks (progression bands) in the region from 1350 to 1180 cm⁻¹, the planarity of the chain segment between the carboxylate group and the double band is found to be dependent upon the surface pressure applied in the process of monolayer transfer onto the germanium plate. Studies of the anisotropy of the absorption index in the films show that the molecules assume a uniaxial orientation with respect to the axis normal to the germanium-sample interface (the *z*-axis), with an angle from 30° to 33° (in average) between the *z*-axis and the molecular axes. Furthermore, from the changes in the reflectivity with the number of layers, the film thickness per layer is estimated to be *ca.* 21.9 Å, a value which is in good agreement with the half-value of the long spacing, 44.16 Å, of the films as determined by X-ray diffraction studies. This apparently indicates that the films appear as the Y type.

Studies on Ion-Exchange Reaction of Metal Salts of Fatty Acids in Alkali-Halide Pellets by Means of Infrared Absorption Spectra. T. Takenaka and R. Gotoh. *Bull. Inst. Chem. Res., Kyoto Univ.*, **50**, 577 (1972).—Infrared spectra of monovalent metal salts of fatty acids were obtained in pellets of various kinds of alkali halides. Variations between the pellet and mull spectra were found in some selective combinations of the metal salts and alkali halides. These changes are due to ion-exchange reaction between the metal salts and alkali halides in the pellets. Factors which influence the reaction are: (1) lattice energy of the alkali halides; (2) energy of grinding mixtures of the metal salts and alkali halides; (3) amount of water contained in the samples; (4) the hydrocarbon-chain length of the metal salts. It is found that the reaction progresses mainly in the course of grinding the mixtures of the metal salts and alkali halides in an agate mortar, and partly in the course of the compression of the mixture in a die.

Coexistence of two Molecular Configurations in Crystalline Carboxylic Acids. S. Hayashi and J. Umemura. *Acta. Cryst.*, **28A**, S239 (1972).—Infrared spectra of benzoic acid and a number of fatty acids were obtained in the range of temperatures from liquid-nitrogen to liquid-helium. Great temperature dependencies

were observed in the regions of the characteristic frequencies of the carboxyl group. The results support the postulate that two distinct equilibrium configurations, which would be led to each other by simultaneous transfer of both protons of the carboxyl groups along the hydrogen bonds, coexist in crystalline state.

Molecular Image Resolution in Electron Microscopy. N. Uyeda, T. Kobayashi, E. Suito, Y. Harada, and M. Watanabe. *J. Applied Physics.*, **43**, 5181 (1972).—High resolution electron microscopy was applied to the epitaxial film of Cu-hexadecachlorophthalocyanine for the achievement of the molecular resolution. In order to define the most suitable direction of observation, the molecular orientation in a crystallite was determined by electron diffraction in advance. The molecular images obtained well reflected the quatre-foiled shape of the individual molecules, although the atomic resolution for each molecule was not attained.

Nucleus Interaction and Fine Structures of Colloidal Gold Particles. N. Uyeda, M. Nishino, and E. Suito. *J. of Colloid and Interface Science*, **43**, 264 (1973).—High resolution electron microscopy was applied to the observation of gold sol particles of several kinds. The anomalous contrasts found in almost all particles indicated that these particles assume various twinned structures of different multiplicities. The formation of such twin structures were ascribed to the regular contact of primary nuclei at the earlier stage of sol formation.

The Nature of Garnierites-II. Electron-Optical Study. N. Uyeda, P. T. Hang, and G. W. Brindley. *Clays and Clay Minerals*, **21**, 41 (1973).—The structure of five kinds of garnierite, Ni-containing clay mineral, were investigated by high resolution electron microscopy. The resolution of layered structures were successfully obtained to show 7 Å and 10 Å lattice images. The former which is considered to assume the talc-type structure appeared to be more regular than the latter which known to have the serpentine-type structure. It was clearly shown that these clay minerals assume deformed tube-like structure or various curled structures.

Layer Structures of Clay Minerals as Revealed by Electron Microscopy. T. Yoshida. *Nendo Kagaku (J. Clay Sci. Japan)*, **13**, 2 (1973), in Japanese.—Layer structures of phlogopite, vermiculite, montmorillonite, organo-montmorillonites and organo-mica/montmorillonite mixed layer mineral were studied by electron microscopy. Many dislocations were observed in the lattice images of layers of the montmorillonite flake.

Electron micrographs of the layers of some organo-montmorillonites showed regular and irregular layer expansion caused by the interlayer adsorption of the organic compounds. Some of the results exhibited local variations of layer expansion even within one particular layer. The local variation was interpreted as due to local differences in exchangeable charge density between the layers.

Effect of a Polar Spreading Solvent on Thin Films. H. E. Ries, *Nature Physical Science*, **243**, 14 (1973).—Many relatively polar film-forming materials require spreading solvents considerably more polar than the hexane, benzene and chloroform

generally used for monolayer spreading. Ethanol has been chosen as a model polar solvent and 1-octadecanol and octadecanoic acid as model film-forming compounds.

Most striking is the small extrapolated area for 1-octadecanol spread from ethanol, 9.8 \AA^2 per molecule, a value close to half that obtained with benzene, 20.4 \AA^2 . Each of three experiments with ethanol gives a slightly higher collapse value, 47 dynes cm^{-1} , than those for three experiments with benzene. Compressibility of the 1-octadecanol film spread from ethanol, 0.0039, is effectively double that for the film spread from benzene, 0.0021. Results obtained with octadecanoic acid parallel those for 1-octadecanol.

The simplest interpretation of these observations is that the films spread from ethanol are two molecules thick. A double-layer structure for such films is consistent with the presence of double-layer platelets or micelles in the spreading solvents.

In double-layer micelles in a relatively nonpolar solvent (benzene), the polar groups of the component molecules are "inside" and the hydrocarbon chains are oriented toward the solvent. When a micellar solution of this type is spread on a water surface, the solvent evaporates and the water moves between the two layers to split open the micelles and to form the normal monolayer. However, in a polar solvent (ethanol), the micelle structure is inverted; that is, the nonpolar hydrocarbon chains are "inside" and the polar groups are oriented toward the solvent (similar to the widely accepted structure of the lipid-bilayer in cell membranes). When such micelles are placed on a water surface, the water molecules have no tendency to penetrate the inner hydrocarbon portion. Thus, the doublelayer micelles formed in ethanol retain their structure at the water surface and the calculated molecular area is half that for the monolayer.

Several additional observations are consistent with the double-layer structure of 1-octadecanol films spread from ethanol. Therefore caution must be exercised in the interpretation of pressure-area isotherms for film-forming compounds spread from polar solvents.

Contact Number and Porosity in Randomly Packed Sphere Mixtures of Various Sizes. M. Arakawa and M. Nishino. *Journal of the Society of Materials Science, Japan*, **22**, 658 (1973), in Japanese.—The relation between contact number and porosity in randomly packed beds of mixtures of various-sized spheres was investigated. The materials used were polystyrene spheres of 1–6 mm in diameter. The spheres were separated by sieving into five size fractions. Three samples having various size distributions were prepared by remixing the appropriate spheres of different size fractions.

The packed beds were prepared by various methods of packing. The porosity values were *ca.* 0.64 for loose packing and *ca.* 0.37 for dense packing. Red ink was poured into the packed bed, filled it up and then drained. The ink was held by capillary force at each contact point after draining. After drying, the marked spheres were separated by sieving into original size fractions, and the distribution of contact numbers was obtained by counting the number of ink marks on each sphere in the same fraction. The contact number in each fraction showed normal distribution, and it increased with increasing particle size and with decreasing porosity. When the

porosity became above 0.45, the relation between the mean contact number and porosity coincided with the result obtained by Ridgway and Tarbuck.

The Influence of Humidity on the Cohesion of Powder Particles. M. Nishino and M. Arakawa. *Journal of the Society of Materials Science, Japan*, **22**, 663 (1973), in Japanese.—In order to investigate the effect of humidity in the atmosphere on the cohesion of powder particles, the adsorption weight of water and the cohesion forces between particles were measured in various humidities. Spherical glass powders with three kinds of particle sizes (17–100 μ) and hydrophobic glass powder made by silicon treatment of the former powders, were used as samples. Cohesive forces were calculated from the tensile strengths of powder beds measured by Du Noüy surface tension balance.

On the basis of the experimental results, it was considered that the water vapor was uniformly adsorbed and formed several water molecular layers on the surface of particles first, and then condensed at the contact points between particles, forming the water bridges. The liquid bridge forces were calculated and compared with the theoretical results by Rumpf.

Standard Powder. M. Arakawa. *Japan Analyst*, **22**, 1260 (1973), in Japanese.—Characteristics of various standard powder for the powder technology have been reviewed.

Recent Research Work in Japan on Particle Size Measurement. M. Arakawa. *J. Res. Assoc. Powder Tech.*, **9**, 81 (1972).—Review.

Inorganic Chemistry

Growth of Crystals Out of Silver-Containing Glass under Electron Bombardment. T. Yamamoto and M. Tashiro. *Bull. Inst. Chem. Res., Kyoto Univ.*, **50**, 591 (1972).—Needlelike crystals grew from a fresh fragment of a silver-containing sodium silicate glass bombarded with intense electron beams in an electron microscope. When the fragment was allowed to stand under a normal atmospheric condition for a week before subjected to the electron bombardment, a little curved rodlike crystals grew from the glass. Electron bombardment caused the formation of colloidal silver within the rodlike crystals.

Loss of Ag and Cl from Photochromic Glasses during Melting in Various Atmospheres. T. Maki and M. Tashiro. *Bull. Inst. Chem. Res., Kyoto Univ.*, **50**, 596 (1972).—The processes of loss of Ag and Cl from photochromic glass batches during melting has been investigated. They were classified into three due to liquid phase separation, vaporization of chlorides from the glass melts and oxidation of chlorides by air. Effects of presence of chloride vapors in the melting atmosphere on the amounts of Ag and Cl remained in the glasses were also examined. When melted in the atmosphere saturated with AgCl, the Ag content of the glass increased rapidly with time, whereas its Cl content remained unchanged.

Effects of Al_2O_3 Addition on Glassy Phase Separation and Crystallization of a $\text{PbO-TiO}_2\text{-SiO}_2$ Glass. T. Kokubo, K. Yamashita, and M. Tashiro. *Bull. Inst. Chem. Res., Kyoto Univ.*, **50**, 608 (1972).—The crystallization processes of the PbO 40, TiO_2 25, SiO_2 35 mole % glass and PbO 40, TiO_2 25, Al_2O_3 10, SiO_2 25 mole % glass were investigated in detail by DTA, electrical resistivity measurement, X-ray diffraction analysis, electron microscopic observation, infrared spectroscopic analysis and fluorescent X-ray spectroscopic analysis. It was found that the former crystallizes directly forming a metastable pyrochlore-type lead titanate, whereas the latter forms the perovskite-type PbTiO_3 crystals via a glassy two-phase separation. It is concluded that addition of the Al_2O_3 to a $\text{PbO-TiO}_2\text{-SiO}_2$ glass induces a glassy two-phase separation, and as the result promotes precipitation of the perovskite-type PbTiO_3 crystal, thus suppressing formation of the metastable crystal.

Effects of Various Manufacturing Conditions on Darkening and Fading of Photochromic Glasses. T. Maki and M. Tashiro. *Bull. Inst. Chem. Res., Kyoto Univ.*, **50**, 621 (1972).—Effects of melting time, heat-treatment time, and γ -ray irradiation before heat treatment on darkening and fading of a photochromic glass were investigated. It was found that the degree of darkening was determined principally by the amount of AgCl crystal particles precipitated in the glass and the absorption coefficient of the particles. The latter showed the maximum when the particle diameter was about 400 Å. The fading rate was high for the specimens which exhibited the strong absorbance after the completion of U. V. illumination.

Loss of Ag and Cl from Photochromic Glasses during Melting in Various Atmospheres. T. Maki and M. Tashiro. *Yogyo-kyokai-shi*, **80**, 417 (1972), in Japanese.—The processes of loss of Ag and Cl from photochromic glass batches during melting has been investigated. They were classified into three due to liquid phase separation, vaporizations of chlorides from the glass melts and oxidation of chlorides by air. Effects of presence of chloride vapors in the melting atmosphere on the amounts of Ag and Cl remained in the glasses were also examined. When melted in the atmosphere saturated with AgCl , the Ag content of the glass increased rapidly with time, whereas its Cl content remained unchanged.

Effects of Al_2O_3 Addition on Glassy Phase Separation and Crystallization of a $\text{PbO-TiO}_2\text{-SiO}_2$ Glass. T. Kokubo, K. Yamashita, and M. Tashiro. *Yogyo-Kyokai-Shi*, **81**, 132 (1973), in Japanese.—The crystallization processes of the PbO 40, TiO_2 25, SiO_2 35 mol % glass and PbO 40, TiO_2 25, Al_2O_3 10, SiO_2 25 mol % glass were investigated in detail by DTA, electrical resistivity measurement, X-ray diffraction analysis, electron microscopic observation, infrared spectroscopic analysis and fluorescent X-ray spectroscopic analysis. It was found that the former crystallizes directly forming a metastable pyrochlore-type lead titanate, whereas the latter forms the perovskite-type PbTiO_3 crystals via a glassy two-phase separation. It is concluded that addition of the Al_2O_3 to a $\text{PbO-TiO}_2\text{-SiO}_2$ glass induces a glassy two-phase separation, and as the result promotes precipitation of the perovskite-type PbTiO_3 crystal, thus suppressing formation of the metastable crystal.

Formation of Defects in Glass under Electron Bombardment. T. Ya-

mamoto, S. Sakka, and M. Tashiro. *J. Amer. Ceram. Soc.*, **55**, 473 (1972).—Needlelike crystals grew from a fragment of glass bombarded with intense electron beams in an electron microscope. This phenomenon was limited to glasses containing mobile atoms such as Na and Pb, to fresh surfaces, and to the part of the sample not coated with carbon film. When there was a relatively thick carbon film on the surface, prolonged electron bombardment caused the formation of bubbles within the fragments.

Advances in Glass Materials. M. Tashiro. *J. Soc. Materials Sci., Japan*, **21**, 817 (1972), in Japanese—Review.

Rate of Homogeneous Nucleation in Alkali Disilicate Glasses. K. Matusita and M. Tashiro. *J. Non-Crystalline Solids*, **11**, 471 (1973).—Rates of crystal nucleation in alkali disilicate glasses were measured by counting the number of crystals under an optical microscope. The viscosities of these glasses were measured by the method of beam-bending and penetration. Using the data of rate of nucleation and viscosity obtained in the present study and the data of free energy measured by Takahashi and Yoshio, crystal-glass interfacial energies for alkali disilicate systems were estimated on the basis of homogeneous nucleation theory as follows; 196 erg/cm² for Li₂O·2SiO₂, 126–144 erg/cm² for Na₂O·2SiO₂ and 88–104 erg/cm² for K₂O·2SiO₂. The effects of the viscosity of glass, the free energy difference between crystal and glass and crystal-glass interfacial energy on the rate of nucleation were discussed, and the remarkably higher rate of crystal nucleation in the Li₂O·2SiO₂ glass was attributed to the larger free energy difference.

Conditions Favorable for the Formation of γ -FeOOH by Aerial Oxidation in an Acidic Suspension of Iron Metal Powder. M. Kiyama, T. Akita, S. Shimizu, Y. Okuda, and T. Takada. *Bull. Chem. Soc. Japan*, **45**, 3422 (1972).—Dilute solutions of ferrous sulfate, sulfuric acid, hydrochloric acid, nitric acid and acetic acid in which iron powders are dispersed have been oxidized at below 80°C by blowing air into them. The resulting precipitates have been examined by means of X-ray diffraction, chemical analysis and optical and electron microscopy. When the iron powder is well dispersed, γ -FeOOH is formed with or without α -FeOOH, α -Fe₂O₃, or Fe₃O₄. The mode of formation depends on such factors as particle size, amount of iron powder, kind of anion present and temperature. Particle size greatly influences the formation of γ -FeOOH in the sulfate system, but not in the other systems.

Mössbauer Study of the Thermal Decomposition Products of K₂FeO₄. T. Ichida. *Bull. Chem. Soc. Japan*, **46**, 79 (1973).—The thermal decomposition process of a hexavalent iron compound, K₂FeO₄, was studied by means of the Mössbauer effect. The compound began to decompose in air at about 170°C, and an amorphous product was obtained by the decomposition below 200°C. The product showed a paramagnetic Mössbauer spectrum at 293°K, with an isomer shift and quadrupole splitting of $+0.40 \pm 0.02$ mm/sec and 0.64 ± 0.02 mm/sec respectively; it also showed a magnetically-split six-line spectrum at 4.2°K, with an internal magnetic field of 480 ± 5 kOe. These Mössbauer parameters are characteristic of the Fe³⁺ state. The intermediate valence states, Fe⁴⁺ or Fe⁴⁺, were not observed during the de-

composition process, and so it was concluded that the Fe^{6+} ions in K_2FeO_4 were reduced directly to Fe^{3+} ions. KFeO_2 was formed in air above 250°C , and the temperature dependence of the internal magnetic field showed the Néel temperature of KFeO_2 to be very high, $983 \pm 10^\circ\text{K}$.

The Effect of the Addition of γ -FeOOH Nuclei at the Initial Stage of Oxidation on the Formation of γ -FeOOH. M. Kiyama, N. Jikuhara, and T. Takada. *Bull. Chem. Soc. Japan*, **46**, 323 (1973).—Acidic solutions containing FeCl_2 and excess NaI were slowly oxidized at below 80°C . α -, β -, γ -FeOOH and α - Fe_2O_3 are precipitated, depending on oxidizing temperature. A mixture of α -FeOOH and γ -FeOOH is precipitated at 60 – 70°C . In this case, the addition of a slight amount of γ -FeOOH nuclei in the starting solution favorably affects the formation of γ -FeOOH by oxidation. It is suggested that γ -FeOOH is formed by an epitaxial reaction of γ -FeOOH nucleus and hydroxo ferric complexes formed by oxidation.

Mössbauer Study of the Thermal Decomposition Products of SrFeO_4 . T. Ichida. *Bull. Chem. Soc. Japan*, **46**, 1591 (1973).—The thermal decomposition products of SrFeO_4 were studied by ^{57}Fe -Mössbauer-effect and X-ray diffraction measurements. Below 300°C in air, an amorphous Fe^{3+} product was formed. The Fe^{4+} or Fe^{5+} state was not observed in the process. A single-phase product with a perovskite structure was obtained in air at temperatures above 400°C . The products obtained between 400 and 650°C showed cubic symmetry, but above 700°C they showed tetragonal distortion. Two kinds of Fe^{3+} -ion sites were detected in the tetragonal SrFeO_x compounds. All the products obtained under the oxygen pressures from 50 to 500 atm and at temperatures from 300 to 900°C showed cubic symmetry. The $\text{Fe}_{3+}/\text{Fe}_{4+}$ ratio in those products was determined from the relative intensities of the Mössbauer absorptions.

The Hydrolysis of Ferric Complexes. Magnetic and Spectrophotometric Studies of Aqueous Solutions of Ferric Salts. M. Kiyama and T. Takada. *Bull. Chem. Soc. Japan*, **46**, 1680 (1973).—Ferric chloro, ferric aquo, and ferric sulfato complexes in acidic solutions have been hydrolyzed at temperatures below 70°C to form polynuclear complexes of iron(III). Magnetic and spectrophotometric studies have then been carried out in order to clarify the nature of the polynuclear complexes. From these studies, their empirical formulas are presumed to be $\text{Fe}_2(\text{OH})_2\text{Cl}_2\text{O}$, $\text{Fe}_2(\text{OH})_3(\text{NO}_3)_3$, $\text{Fe}_2(\text{OH})_3(\text{SO}_4)_{3/2}$, and $\text{Fe}_3(\text{OH})_2(\text{SO}_4)_{7/2}$. The iron ions in these polynuclear complexes are in a high spin state, as are those in the ferric complexes, iron oxides, and oxyhydrates. It is proposed that, in all these polynuclear complexes except $\text{Fe}_3(\text{OH})_2(\text{SO}_4)_{7/2}$, edge-shared octahedral dimer units are antiferromagnetically linked with one another by hydroxy or oxo bridging. When the hydrolysis temperature is raised, these polynuclear complexes are further hydrolyzed to form precipitates. The complexes of $\text{Fe}_2(\text{OH})_2\text{Cl}_2\text{O}$, $\text{Fe}_2(\text{OH})_3(\text{SO}_4)_{3/2}$, $\text{Fe}_3(\text{OH})_2(\text{SO}_4)_{7/2}$ give β -FeOOH, α -FeOOH, and $\text{RFe}_3(\text{OH})_6(\text{SO}_4)_2$ ($\text{R}=\text{Na}$, K or NH_4) respectively, whereas the complex of $\text{Fe}_2(\text{OH})_3(\text{NO}_3)_3$ gives α -FeOOH or α - Fe_2O_3 , depending on the temperature.

Mössbauer Effect Study of Fe⁵⁷ Doped in the V_nO_{2n-1} System. H. Okinaka, K. Kosuge, S. Kachi, M. Takano, and T. Takada. *J. Phys. Soc. Japan*, **32**, 1148 (1972).—It was found from the Mössbauer spectra that all the sample of V₃O₄, V₄O₇ and V₇O₁₃ are antiferromagnetic at 4.2 K. The internal fields of Fe⁵⁷ in V₃O₅, V₄O₇ and V₇O₁₃ at 4.2 K are about 390, 400 and 440 kOe, respectively. The internal field, in cases of V₄O₇ and V₇O₁₃ phase, decrease with increasing temperature and disappear near to (40 K in V₄O₇ and 43 K in V₇O₁₃), at which magnetic susceptibility shows an anomalous peak.

Mössbauer Study on the Magnetism of Trinuclear Complex Salts. M. Takano. *J. Phys. Soc. Japan*, **33**, 1312 (1972).—A susceptibility measurement on [Fe₃O(CH₃COO)₆(H₂O)₃]Cl·6H₂O at temperatures between 4.2 K and 1.3 K shows that the triangular Fe³⁺-clusters have spin 1/2 in the ground state owing to strong antiferromagnetic intracluster interactions. The Mössbauer spectrum of this salt in the external field of 50 kOe at 1.5 K consists of three sets of magnetically split patterns with the effective fields of 210 kOe, 175 kOe and 80 kOe, respectively. The spectrum from the (Cr₂Fe)-clusters in the isomorphous Cr-salt with Fe⁵⁷ substituting for Cr³⁺ ions up to 2% has a single pattern with the effective field of 235 kOe. It is shown that antiferromagnetic intracluster interactions cause the constituent Fe³⁺ (and Cr³⁺) ions to have small positive or negative spin components along the large polarizing field. The three interactions in an Fe-cluster are not equivalent to each other. For a (Cr₂Fe)-cluster, the Fe³⁺-Cr³⁺ interactions are stronger than the Cr³⁺-Cr³⁺ one.

A Mössbauer Study of Magnetic Hyperfine Fields in Fe³⁺-Antiferromagnetic Oxides. M. Takano, T. Shinjo, M. Kiyama, and T. Takada. *J. Phys. Soc. Japan*, **35**, 53 (1973).—The single-ion hyperfine fields in Fe³⁺ ions diluted in KAl₃(OH)₆(SO₄)₂, γ-Al₁₀₀H and ZnAl₂O₄ have been measured with the Mössbauer effect in an external magnetic field of 50 kOe at liquid helium temperatures. The values are 570±8 kOe, 565±8 kOe and 550±10 kOe, respectively, while the previously reported hyperfine fields of the corresponding antiferromagnets at OK are 490 kOe, 470 kOe and 515 kOe. The remarkable reductions in KFe₃(OH)₆(SO₄)₂ and γ-FeOOH indicate large spin deviations due to two dimensional antiferromagnetic interactions.

Magnetic Properties of FeTi₂S₄. S. Muranaka. *J. Phys. Soc. Japan*, **35**, 616 (1973).—In order to study the magnetic properties of FeTi₂S₄, magnetic torque and magnetization measurements were carried out using single crystal samples which were prepared by a chemical transport method with Cl₂ as a carrier gas.

Order-Disorder Transition of Vacancies in FeTi₂S₄. S. Muranaka. *Mat. Res. Bull.*, **8**, 679 (1973).—Vacancy-ordered FeTi₂S₄ was prepared by a prolonged heat treatment. X-ray and magnetic measurements showed the transition of vacancies to the disordered state at about 450°C. The magnetic property was antiferromagnetic, having the Néel temperature at 138 K. The increase of ferromagnetic character was associated with the disordering of vacancies.

Mössbauer Effect of FeOCl-Pyridine Complex. F. Kanamaru, M. Shimada, M. Koizumi, M. Takano, and T. Takada. *J. Solid State Chem.*, **7**, 297 (1973).—A Mössbauer effect study has been conducted on FeOCl-pyridine complex in the temperature range between 4.2° and 298°K. The isomer shift relative to Fe metal and the quadrupole splitting at 298°K are 0.36 ± 0.01 and 0.92 ± 0.01 mm/sec, respectively. An antiferromagnetic ordering occurs at $65 \pm 3^\circ\text{K}$. The internal magnetic field is 435 ± 10 kOe at 4.2°K. The z axis of the electric field gradient tensor ($|V_{zz}| > |V_{xx}| \geq |V_{yy}|$, η being small) is shown to be parallel to the direction of the internal magnetic field and perpendicular to the crystalline b axis.

Crystal Growth of Vanadium Oxides by Chemical Transport. K. Nagasawa. *J. Cryst. Growth*, **17**, 143 (1972).—Single crystals of VO_2 , V_2O_3 and the intermediate vanadium oxides between VO_2 and V_2O_3 with the general formula $\text{V}_n\text{O}_{2n-1}$ ($n=3,4,5,6,7,8$) were grown by the chemical transport using TeCl_4 as a transport agent. The crystallography of $\text{V}_n\text{O}_{2n-1}$ and the electrical properties of the grown crystals are studied. Some related topics are also reviewed.

Growth of Mn_3O_4 Single Crystals by Chemical Transport Method. N. Yamamoto, K. Nagasawa, Y. Bando, and T. Takada. *Japan. J. Appl. Phys.*, **11**, 1754 (1972).—The single crystals of Mn_3O_4 were grown by Chemical Transport Reaction using HCl or Cl_2 gas as transport agent. The crystals were rod-shaped and their longest axis were parallel to the $[100]$ axis of b.c.t. unit cell.

An Introduction to Mössbauer Spectroscopy. T. Shinjo. *Kagaku*, **27**, 952 (1972), in Japanese.—A brief introduction to Mössbauer spectroscopy was presented with explaining some examples of actual spectra. It was emphasized that the measurements were very easy and the interpretation of the results was not difficult.

Topotaxy in Solid State Reaction. Y. Bando. *Chemistry*, **27**, 995 (1972), in Japanese.—Review; Topotactic reaction in decomposition of hydroxide and spinel formation were discussed.

Preparation of Oxides by Chemical Vapor Deposition. Y. Bando. *Electronic Ceramics*, **4**, 29 (1973), in Japanese.—Review; The growth of single crystals and thin film of oxides by chemical vapor deposition were reviewed. The magnetic properties of thin film were also discussed.

Heat Capacity Anomaly in the Crystalline Organic Free Radical, p-Cl-BDPA. J. Yamauchi, K. Adachi, and Y. Deguchi. *Chem. Letters*, 733 (1972). The heat capacity has been measured on polycrystalline sample of 1,3-bisdiphenylene-2-p-chlorophenyl-allyl (abbreviated as p-Cl-BDPA). The sharp heat capacity anomaly was observed at 3.25 K, which may imply a paramagnetic-antiferromagnetic phase transition. This phenomenon accords well with the other results obtained from the susceptibility, ESR, and NMR measurements. The detail of this paper was published in *J. Phys. Soc. Japan*, **35**, 443 (1973).

Dipolar Interaction in TEMPAD Biradical. J. Yamauchi, T. Fujito, A. Nakajima, H. O. Nishiguchi, and Y. Deguchi. *Bull. Chem. Soc. Japan*, **44**, 2263 (1971).—In TEMPAD, bis-2,2,6,6-tetramethylpiperidine-4-azine-1,1'-dioxyl, biradical the dipolar interaction was found by reducing the exchange interaction between triplet excitons at lower temperatures. The ESR spectra showed a newly-appeared doublet absorption, the spacing being evaluated as 76.6 gauss. The average distance between the unpaired electrons is nearly 8 Å, which is quite well in accord with the distance between the unpaired electrons in a molecule, that is 9 Å. It can be ascribed to the intramolecular interaction between the unpaired electrons in a molecule.

Linear Antiferromagnetic Interaction in Organic Free Radicals. J. Yamauchi. *Bull. Chem. Soc. Japan*, **44**, 2301 (1971).—The static magnetic susceptibilities from 1.8°K to 300°K, and the ESR spectra from 1.5°K to 300°K, of several organic free radicals have been measured on powder samples. The broad maxima in the susceptibility which indicate the antiferromagnetic interaction and the broadening of the ESR absorption lines have been observed. The data are analysed on the basis of the linear Heisenberg model and shown to be consistent with the one-dimensional magnetic chain model of isotropic exchange interaction. Discussions are made of the grounds of susceptibility, the ESR, and the specific heat measurements. In addition to a short-range ordering of spins, the possibility of long-range ordering is also discussed in two radicals, BDPA-Bz and *p*-Cl-BDPA, on the basis of discontinuities in the slope of susceptibility, the rapid broadening of the ESR linewidth, and the disappearance of the ESR absorption.

Magnetic properties of Organic Stable Radicals. III. Diphenyl Nitric Oxide. O. Takizawa, J. Yamauchi, H. O. Nishiguchi, and Y. Deguchi. *Bull. Chem. Soc. Japan*, **44**, 3188 (1971).—In the present paper the results of the susceptibility measurement of diphenyl nitric oxide (DPNO) was reported. DPNO shows a broad maximum in the susceptibility at 6.2°K and has Weiss constant of -3.5°K , which indicates an antiferromagnetic interaction in the electron spins in the molecules. The data were analysed using the one-dimensional Heisenberg model with $T_m = 6.2^{\circ}\text{K}$. The theoretical results agree well with the present experimental results in the available temperature region.

Abnormal Hyperfine Splitting in the ESR Spectra of 1,1,3,3-Tetraphenylallyl-type Organic Stable Free Radicals. K. Watanabe, J. Yamauchi, H. Nishiguchi, Y. Deguchi, and H. Takaki. *Bull. Chem. Soc. Japan*, **45**, 371 (1972).—The ESR spectra of 1,1,3,3-tetraphenylallyl radical have been first observed. An abnormal ESR hyperfine splitting of this radical has been compared with the ESR hyperfine splitting of other tetraphenylallyl-type radicals. The mechanism of this abnormal hyperfine splitting was discussed in detail. It can be explained very well by introducing the idea of a twisted-allyl model of the molecule.

Magnetic Properties of 2,2,6,6-Tetramethyl-4-Hydroxypiperidine-1-Oxyl-4-Derivatives. J. Yamauchi, K. Watanabe, H. Nishiguchi, and Y. Deguchi. *Bull. Inst. Chem. Res., Kyoto Univ.*, **50**, 483 (1972).—The magnetic susceptibilities of

TANOL and 4-substituted TANOL derivatives were observed in the temperature region from 1.8°K to 300°K. The Weiss constants are determined to be 0°K for methyl and ethyl, -1.5°K for isopropyl and tert-butyl, -1.0°K for phenyl, -2.5°K for cyclohexyl derivatives, and -6.0°K for TANOL. The temperature, T_m , which is proportional to the exchange interaction parameter, J , is roughly estimated to be 6.5°K for TANOL, 1.5 K for cyclohexyl, and 1°K for phenyl derivatives. Besides, the O-H vibration band in infrared absorption spectra was also observed in the radicals where the hydrogen bond is anticipated to be formed along a crystallographic **a**-axis. The effect of the substituents to the exchange interaction was discussed and it is concluded that the results are not contradictory to the assumption that TANOL may have a linear exchange interaction along **c**-axis.

Organic Chemistry

Oxidation Involved in Organometallic Reactions. K. Ichikawa and S. Uemura. *Bull. Inst. Chem. Res., Kyoto Univ.*, **50**, 225 (1972).—Results, obtained on the oxidation involved in organometallic reactions, have been classified into S_N1 and S_N2 type, oxidative substitution in aromatics, oxidative coupling and oxidative addition. Major interests are in the reactions of Hg, Tl, Cu and Pd compounds. Related results reported in the literature are also reviewed briefly.

Liquid Phase Halogenation with Metal Halides. S. Uemura and M. Okano. *Bull. Inst. Chem. Res., Kyoto Univ.*, **50**, 423 (1972).—Recent studies on the liquid phase halogenation of alkanes, olefins, acetylenes, and arenes with metal or metalloidal halides are reviewed. Some characteristics in these halogenation reactions, as compared with halogenation by molecular halogens, are mentioned.

Concurrent Chlorination and Carboxylation of Aromatic Hydrocarbons with Thallium(III) Chloride Tetrahydrate in Carbon Tetrachloride. S. Uemura, O. Sasaki, and M. Okano. *J. Chem. Soc., Perkin I*, 2268 (1972).—In contrast to aromatic bromination with $TlBr_3 \cdot 4H_2O$, the reaction of lower aromatic hydrocarbons (C_6 - C_8) with molten $TlCl_3 \cdot 4H_2O$ in boiling carbon tetrachloride afforded the corresponding benzoic acids together with the expected chlorinated aromatic compounds. At lower temperatures, carboxylation was considerably favoured. Possible mechanisms for chlorination and carboxylation have been discussed.

Substitution of Thallium with Halogen in the Reaction of Arylthallium(III) Compounds with Copper Halides. S. Uemura, Y. Ikeda, and K. Ichikawa. *Tetrahedron*, **28**, 5499 (1972).—The reaction of arylthallium(III) compounds with copper(II) and (I) halides was found to afford aromatic hydrocarbons, aromatic halides and aromatic coupling products in various organic solvents. Choice of solvent had a remarkable effect on the yields and the product distributions, dioxane being the solvent of choice for the purpose of preparing aromatic halides. The aromatic halide formation is explained by an ionic concerted intermolecular mechanism.

Reaction of Alkylphenylenes with Thallium(III) Acetate. S. Uemura, K. Sohma, H. Tara, and M. Okano. *Chemistry Letters*, 545 (1973).—The reaction of alkylphenylacetylenes with thallium(III) acetate in acetic acid under mild conditions (at 60–70°C for 1 hr) afforded a mixture of two isomeric acetoxythallated compounds in good yields. The hydrodethallation of these products to give the corresponding vinyl acetates was accomplished with boiling acetic acid.

Terpenoids. XX. The Structure and Absolute Configuration of Lasiokaurin and Lasiodonin, New Diterpenoids from *Isodon lasiocarpus* (HAYATA) KUDO E. Fujita and M. Taoka. *Chem. Pharm. Bull. (Tokyo)*, **20**, 1752 (1972).—On the basis of chemical and spectroscopic evidence, the structure and absolute configuration of lasiokaurin and lasiodonin, which were isolated from *Isodon lasiocarpus* (HAYATA) KUDO, were established as *ent*-7 β ,20-epoxy-1 β -acetoxy-15-oxo-16-kaurene-6a,7 a, 14 a-triol and *ent*-7 β ,20-epoxy-15-oxo-16-kaurene-1 β ,6 a,7 a,11 a-tetraol, respectively.

Terpenoids. XXI. The Structure and Stereochemistry of Isodotricin, a Diterpenoid of *Isodon trichocarpus* and *I. japonicus*. E. Fujita, T. Fujita, Y. Okada, S. Nakamura, and M. Shibuya. *Chem. Pharm. Bull.*, **20**, 2377 (1972).—The structure of isodotricin, a diterpenoid of *Isodon trichocarpus* and *I. japonicus*, was determined by a chemical conversion from enmein. The more detailed investigation on the stereochemistry of C-16 led to a conclusion for the S-configuration, thus, the structure and absolute configuration of isodotricin were established.

Change of Quantity of Each Major Diterpenoid During Growth of *Isodon trichocarpus* KUDO Its Exploration by GC and GC-MS. E. Fujita, Y. Nagao, S. Nakano, Y. Masada, K. Hashimoto, and T. Inoue. *Yakugaku Zasshi*, **92**, 1400 (1972), in Japanese.—As a preliminary experiment of the biosynthesis, changes in the quantity of major diterpenoids during growth of *Isodon trichocarpus* KUDO were examined by gas chromatography and the combined gas chromatography-mass spectrometry (GC-MS). A change in the quantity was found by plotting the area ratio of trimethylsilylated diterpenoids to that of internal standard in gas chromatography every 10 days. Enmein and oridonin showed a similar tendency of changes in their quantity. They were found to increase markedly in June and July.

Terpenoids. XXIII. Reduction of Kaurene with Hydrazine and Hydrazine Hydrochloride. E. Fujita and Y. Nagao. *Yakugaku Zasshi*, **92**, 1405 (1972), in Japanese.—It was found that Wolff-Kishner reduction of *ent*-15-kauren-6-on-20-al, using hydrazine hydrochloride, 98.5% hydrazine, and potassium hydroxide in triethyleneglycol (Nagata's modification), gave only *ent*-kaurane, a product accompanied by the stereoselective hydrogenation of the double bond between C-15 and C-16. Various experiments using *ent*-16-kaurene as a model compound showed that (i) hydrogenation from *ent*-16-kaurene to *ent*-kaurane readily occurred by hydrazine and its hydrochloride in air, (ii) it occurred even with only hydrazine in air, but not in nitrogen, and that (iii) it occurred in the presence of hydrazine hydro-

chloride even in nitrogen, although the yield was rather poor. The possible mechanisms were discussed.

Terpenoids. XXIV. Isolation of Isodonal and Epinodosin from *Isodon japonicus* and Structure Elucidation of Sodoaponin and Epinodosinol, Novel Diterpenoids of the Same Plant. E. Fujita, T. Fujita, M. Taoka, H. Katayama, and M. Shibuya. *Chem. Pharm. Bull.*, **21**, 1357 (1973).—Four diterpenoids were isolated from the dried leaves and stems of *Isodon japonicus* HARA. Two of them were shown to be identical with the known isodonal and epinodosin. Spectroscopic investigation and a chemical conversion into epinodosin dihydroderivative established the structure and absolute configuration of sodoaponin. The structure and absolute configuration of epinodosinol were elucidated, on the basis of spectroscopic data and some chemical evidence. Finally, sodoaponin was converted into epinodosinol, which confirmed their structures unequivocally.

Lythraceous Alkaloids. Part VI. The Structures of Lythrancine-I, -II, -III, and -IV and Lythrancepine-I, -II, and -III. E. Fujita and Y. Saeki. *J. C. S. Perkin I*, 2142 (1972).—Chemical and spectroscopic investigation of seven new *Lythrum* alkaloids, lythrancine-I, -II, -III, and -IV, and lythrancepine-I, -II, and -III, led to elucidation of their structures. All were shown to have a common basic structure of 4-(biphenyl-3-yl)-perhydroquinolizine with a butane bridge between the 3'-position of the biphenyl group and the 6-position of the quinolizine nucleus.

Lythraceous Alkaloids. Part VII. The Absolute Configurations of Lythrancines-I—IV and Lythrancepines-I—III. E. Fujita and Y. Saeki. *J. C. S. Perkin I*, 297 (1973).—An n.m.r. investigation of lythrancine-IV provided evidence for a *cis*-relationship among 1-, 3-, and 4-H, and of a *cis*-ring-functure of the quinolizidine ring. The chemical conversion of lythrancepine-II into a lythranidine-type triformate, which was proved to be the antipode of the same compound derived from lythranidine, established the absolute configuration of C-5, -9, and -11. Consideration of this result together with the relative stereochemistry of C-1, -3, and -4 led to two possible stereostructures. Use of a stereomodel showed a preference for one of them. X-ray analysis of lythrancine-II-*O*-brosylate rigorously confirmed this assumption. The absolute stereochemistry of the seven new bases, lythrancines-I—IV and lythrancepines-I—III was thus established.

Lythraceous Alkaloids. Part VIII. The Mass Spectra of Lythrancine and Lythrancepine Alkaloids. E. Fujita and Y. Saeki. *J. C. S. Perkin I*, 301 (1973).—The mass spectra of the quinolizidine alkaloids isolated from *Lythrum anceps* MAKINO and their derivatives were taken. The fragmentation mechanism was investigated and the location of hydroxy- or acetoxy-substituent(s) at C-3, -4, and -11 was established.

Lythraceous Alkaloids. Part IX. The Structure and Absolute Configuration of Lythrancine-V, -VI, and -VII. E. Fujita and Y. Saeki. *J. C. S. Perkin I*, 306 (1973).—Three minor alkaloids, lythrancine-V, -VI, and -VII were

isolated from *Lythrum anceps* MAKINO. Lythrancine-V is the C-3 epimer of lythrancine-IV. Lythrancine-VI and -VII are the deacetyl derivatives of lythrancine-V. Mass spectral data and a chemical conversion of lythrancine-III into lythrancine-V gave their structure and absolute configuration.

Investigation of the Neutral Constituents of *Lythrum Salicaria* L. E. Fujita, Y. Sacki, M. Ochiai, and T. Inoue. *Bull. Inst. Chem. Res, Kyoto Univ.*, **50**, 327 (1972).—Isolation and characterization of di-isobutyl, *n*- and *iso*-butyl, and di-*n*-butyl phthalate, β -sitosterol, and loliolide from the methanol extract of the whole herb of *Lythrum Salicaria* L are described. Detections of dioctyl phthalate, four new diheptyl phthalates, and two new dinonyl phthalates by the combined gas chromatography-mass spectrometry are also described.

Investigation of the Non-basic Constituents of *Lythrum anceps* MAKINO. E. Fujita, K. Fuji, S. Nakamura, and Y. Takaishi. *Bull. Inst. Chem. Res., Kyoto Univ.*, **50**, 206 (1972).—Investigation of the non-basic constituents of *Lythrum anceps* MAKINO led to isolation and characterization of ellagic acid and betulic acid.

Total Synthesis of Enmein. E. Fujita, M. Shibuya, S. Nakamura, Y. Okada, and T. Fujita. *J. C. S. Chem. Comm.*, 1107 (1972).—A total synthesis of enmein was accomplished by a transformation of the previously synthesized relay compound.

New Phenolic Hasubanan Alkaloids from *Stephania abyssinica*. S. M. Kupchan, A. J. Liepa, and T. Fujita. *J. Org. Chem.*, **38**, 151 (1973).—Three new alkaloids, stephabyssine, stephaboline, and prostephabyssine, were isolated from *Stephania abyssinica* WALP. They have a phenolic hasubanan nucleus. The assignments of the structures were based on the spectral data and some chemical evidences.

The Isolation and Structural Elucidation of Eupaserrin and Deacetyl-eupaserrin, New Antileukemic Sesquiterpene Lactones from *Eupatorium semiserratatum*. S. M. Kupchan, T. Fujita, M. Maruyama, and R. W. Britton. *J. Org. Chem.*, **38**, 1260 (1973).—Two new antileukemic sesquiterpene lactones, eupaserrin and deacetylepupaserrin, were isolated from *Eupatorium semiseratum* DC., and their structure was elucidated on the basis of the chemical and spectral evidence.

Structural Elucidation of Novel Tumor-Inhibitory Sesquiterpene Lactones from *Eupatorium cuneifolium*. S. M. Kupchan, M. Maruyama, R. J. Hemingway, J. C. Hemingway, S. Shibuya, and T. Fujita. *J. Org. Chem.*, **38**, 2189 (1973).—Five new cytotoxic germacranolide lactones were isolated from *Eupatorium cuneifolium* WILLD. The structures of eupacunin (1) and eupacunoxin (2) were elaborated by chemical and spectral arguments, and confirmed by X-ray crystallographic analysis of their bromo derivatives, respectively. Eupatocunin was interrelated with 1 by conversion of each to the epoxyketone. The structure of eupatocunoxin, isomeric with 2, was determined on the basis of spectral arguments. Eupacunolin was characterized as a hydroxy eupacunin. The most abundant lactone, eupacunin, was tested *in vivo* and was found to show inhibitory activity against the leukemia in mice and the carcinosacoma in rats.

The Isolation and Structural Elucidation of Liatrin, a Novel Antileukemic Sesquiterpene Lactone from *Liatris chapmanii*. S. M. Kupchan, V. H. Davies, T. Fujita, R. Cox, R. J. Restivo, and R. F. Bryan. *J. Org. Chem.*, **38**, 1853 (1973).—The isolation and structural elucidation of liatrin, a novel sesquiterpene lactone from *Liatris chapmanii*, are reported. Liatrin has significant antileukemic activity in mice and possesses the unusual germacranolide *cis*, *cis*-diene structure. The structure of liatrin was established by X-ray crystallographic analysis of the bromo derivative and some chemical reactions.

The Synthesis of Methylacetylene by the Pyrolysis of Propylene. (VII).
The Catalysis of Iodine. M. Taniuchi. *Bull. Inst. Chem. Res., Kyoto Univ.*, **50**, 383 (1972).—The pyrolysis of propylene in the presence of iodine was studied in a flow system with a nitrogen dilution over a wide range of conditions (temperature, 800–1200°C; contact time, 0.774×10^{-3} – 490×10^{-3} sec; pressure, atmospheric pressure) in order to find suitable conditions for producing methylacetylene and allene, and to obtain data concerning the distribution of the pyrolysis products. Iodine promoted the rate of propylene pyrolysis and the concentration of iodine affected the product distribution. The main products of the pyrolysis were found to be hydrogen, methane, acetylene, ethylene, allene, methylacetylene, butadiene, benzene, and isopropyl iodide. The total yield of methylacetylene and allene of 46 mol per 100 mol propylene pyrolyzed was attained under suitable conditions. It was further found that small amounts of iodine (*ca.* 0.3 mol% of iodine for 13 mol% of propylene) were very effective for the synthesis of methylacetylene and allene at high temperatures (around 1200°C) and that the catalytic effect of iodine was considerably remarkable even at higher conversions. A brief discussion is given of the formation of methylacetylene and the catalytic effect of iodine.

The Synthesis of Methylacetylene by the Pyrolysis of Propylene. (VIII)
The Pyrolysis of Allyl Bromide. S. Kunichika, Y. Sakakibara, M. Taniuchi, and R. Okuda. *Bull. Inst. Chem. Res., Kyoto Univ.*, **50**, 393 (1972).—Allyl bromide has been pyrolysed in a flow system with a nitrogen dilution over a wide range of conditions (temperature, 800–1200°C; contact time, 0.188×10^{-3} – 2.30×10^{-3} sec; concentration, 3.2–9.5 mol%; pressure, atmospheric pressure) in order to elucidate the pyrolytic behaviors of allyl bromide at high temperatures. The main products in the pyrolysis were found to be hydrogen, methane, ethane, ethylene, acetylene, allene, methylacetylene, propylene, butadiene, benzene, diallyl, *n*-propyl bromide, and 1-bromopropene. By means of the zero-conversion method, it has been shown that, among them, hydrogen, ethylene, allene, propylene, butadiene, benzene, and diallyl are the major products in the early stage of the pyrolysis. On the basis of the observed results, a free radical mechanism has been proposed for the main and the principal side reactions. It has further been concluded that the pyrolysis is a radical decomposition initiated by the reaction $C_3H_5Br \rightarrow C_3H_5\cdot + Br$ and that the mechanism in the early stage of the pyrolysis is explained essentially by the reactions of allyl radicals and bromoallyl radicals.

Friedel-Crafts Aralkylation III. The Reaction of Benzene with 2-Phenylethyl-1,1-d₂ and 2-(p-Chlorophenyl)-ethyl-1,1-d₂ Chlorides. M. Ichii, T. Sugiyama, and S. Oka. *Bull. Inst. Chem. Res., Kyoto Univ.*, **50**, 404 (1972).—The AlCl₃·CH₃NO₂-catalyzed phenethylation of benzene with 2-phenylethyl-1,1-d₂ and 2-(p-chlorophenyl)-ethyl-1,1-d₂ chlorides in nitromethane solution has been investigated. In the unreacted chlorides, 1,2-aryl migration was observed and the amounts of 2-arylethyl-2,2-d₂ chlorides formed increased with reaction time. The same extent of the migration was also observed in absence of benzene.

Recent Progress in the Chemistry of Allenes. T. Okamoto. *Bull. Inst. Chem. Res., Kyoto Univ.*, **50**, 450 (1972).—Review.

The Synthesis of Methylacetylene by the Pyrolysis of Propylene (IX). The Mechanism of the Iodine-catalyzed Pyrolysis of Propylene. M. Taniuchi. *Bull. Inst. Chem. Res., Kyoto Univ.*, **50**, 660 (1972).—A study has been made of the mechanism for the pyrolysis of propylene in the presence of iodine at high temperatures (800–1200°C). By means of the zero conversion method, hydrogen, methane, ethylene, and allene have been found to be the main primary products, while methylacetylene, acetylene, and benzene have been found to be the chief secondary products. On the basis of the observed results, a free radical chain mechanism has been proposed for the main reactions. The catalysis of iodine and the product distributions have been satisfactorily explained by this mechanism. The catalytic effect of iodine on the synthesis of methylacetylene and allene is attributable to (1) the reformation of iodine and the iodine atom by the reactions of hydrogen iodide: $2\text{HI} \rightarrow \text{H}_2 + \text{I}_2$, $\text{H} + \text{HI} \rightarrow \text{H}_2 + \text{I}$, $\text{CH}_3 \cdot \text{HI} \rightarrow \text{CH}_4 + \text{I}$; (2) the promotion of formation of the allyl radical from propylene and allene from the allyl radical: $\text{CH}_2 = \text{CH} - \text{CH}_3 + \text{I} \rightarrow \text{CH}_2 = \text{CH} - \text{CH}_2 \cdot + \text{HI}$, $\text{CH}_2 = \text{CH} - \text{CH}_2 \cdot + \text{I} \rightarrow \text{CH}_2 = \text{C} = \text{CH}_2 + \text{HI}$, $\text{CH}_2 = \text{CH} - \text{CH}_2 \cdot + \text{I}_2 \rightarrow \text{CH}_2 = \text{C} = \text{CH}_2 + \text{HI} + \text{I}$; and (3) the suppression of decomposition of propylene to ethylene and the methyl radical: $\text{CH}_2 = \text{CH} - \text{CH}_3 + \text{H} \rightarrow \text{CH}_2 = \text{CH}_2 + \text{CH}_3 \cdot$.

Chlorination of Some Bridge-Substituted Acenaphthenes and Related Compounds. H. Suzuki, K. Kawamura, and T. Sugiyama. *Bull. Inst. Chem. Res., Kyoto Univ.*, **51**, 186 (1973).—Acenaphthene, perinaphthene, and 1,8-dimethylnaphthalene were treated with molecular chlorine in a mixture of carbon tetrachloride and acetic acid (3 : 1, V/V) at 15.0°C. Overall relative reactivities: acenaphthene 8.40, perinaphthene 1.00, 1,8-dimethylnaphthalene 0.38 were determined and ortho: para ratios of the monochloro compounds were found to be almost identical. Relative rates for chlorination of bridge substituted acenaphthenes have also been measured. Substituents on C-1 and C-2 atoms decrease the reaction rate. These results are discussed in terms of a second-order hyperconjugation effect.

The Jacobsen Reaction of Iodopseudocumenes and Related Compounds. Orientation in the Iodination of Halopseudocumenes. H. Suzuki and T. Sugiyama. *Bull. Chem. Soc. Japan*, **46**, 586 (1973).—The Jacobsen reaction of iodopseudocumenes and related compounds was investigated. Both 3- and 5-iodopseudocumenes gave essentially the same product which consisted of 3,5-diiodopseudocumene

(VI, 53%), 3,6-diiodopseudocumene (VII, 44%) and 5,6-diiodopseudocumene (VIII, 3%). The unexpected result was interpreted in terms of a mechanism involving a prior interconversion of the 3- and 5-iodo isomers followed by the ordinary process of aromatic disproportionation. 6-Iodopseudocumene gave VII as the major product. By prolonged contact with concentrated sulfuric acid, VI and VIII were found to undergo partial isomerisation to give VII. Early structural assignment by Smith and Moyle for two diiodopseudocumenes was revised. Reactions of 4- and 5-iodohemimellitenes with sulfuric acid gave 4,6-diiodohemimellitene (XII) as the major product. A diiodohemimellitene melting at 114°C was found to be a mixture of XII and 4,5-diiodohemimellitene (XI), the former being predominant. Isomeric chloro-, bromo-, and iodopseudocumenes were iodinated with iodine-periodic acid dihydrate and the orientation in the products was determined.

Palladium (II) Catalyzed Synthesis of Aryl Cyanides From Aryl Halides.

K. Takaki, T. Okamoto, Y. Sakakibara, and S. Oka. *Chemistry Letters*, 471 (1973).—In the presence of pd(II) salts, substitution reaction of aryl halides with potassium cyanide occurs readily which affords a simple and beneficial method for aryl cyanide synthesis.

Reaction of Chloramines, Part IV. The Reaction of Chloramines with β -Ketoesters and β -Diketones. J. Oda, M. Horiike, and Y. Inouye. *Bull. Inst. Chem. Res., Kyoto Univ.*, **50**, 183 (1972).—The reaction of chloramines with β -ketoesters and β -diketones have been shown to yield the two corresponding fragmentation products, amides and dichloro-derivatives. The results of this study indicates that the reaction is initiated by the addition of chlorinium cation to the enolic carbon-carbon double bond, and subsequent decomposition occurs via dichloroketo-ester or diketone as transient intermediates. The behavior of the carbon-carbon bond fission is characteristic of the varieties of chloramine.

Partial Asymmetric Synthesis of $\Delta^{1,9}$ -2-Octalone with Chiral Enamine.

T. Igarashi, J. Oda, and Y. Inouye. *Bull. Inst. Chem. Res., Kyoto Univ.*, **50**, 222 (1972).—The nucleophilic addition of (–)-(S)-N-methyl- α -phenylaminocyclohexene to methyl vinyl ketone, followed by the intramolecular proton shift and again nucleophilic cyclization, yielded, after work-up, (–)- $\Delta^{1,9}$ -2-octalone. The enantiomeric product was obtained from (+)-(R)-enamine. The absolute configuration of chiral octalone thus obtained was established by means of chiroptical comparison with (–)-(10 α -methyl- $\Delta^{1,9}$ -2-octalone of the well-defined R-configuration. The levorotatory octalone was assigned the R-configuration. The steric course of the present asymmetric reaction was discussed.

Absolute Configuration of Dimethyltartaric Acid. M. Muroi, J. Oda, and Y. Inouye. *Bull. Inst. Chem. Res., Kyoto Univ.*, **51**, 182 (1977).—(+)-2,3-Dimethyltartaric acid was converted to the corresponding (–)-O,O-dianisoyldimethyltartaric acid anhydride and the R-configuration was assigned on the basis of the chiroptical data with the corresponding dianisoyltartaric acid anhydride used as reference. Conformational equilibrium conceivable for these cyclic compounds was discussed in the

light of exciton chirality rule, which was in agreement with the present chiroptical observation.

Optically Active Bis- β -keto Sulfonium Ylid. M. Muroi, Y. Nakajima, J. Oda, and Y. Inouye. *Agr. Biol. Chem.*, **36**, 2045 (1972).—Levorotatory (ethylmethylsulfonium)-p,p'-bisphenacylid was for the first time prepared and isolated pure. After full substantiation of the proposed structure, the chiral bis-sulfonium ylid was allowed to react with two kinds of Michael acceptors to yield the corresponding bis-cyclopropanoids of levorotation respectively. It was shown by the present study that the chirality originally residing on sulfur atoms of the sulfonium salt is retained in the bis-ylid, and upon the reaction with electrophilic olefin substrates, is transferred to trigonal carbon atoms at the expense of the former, to afford chiral bis-cyclopropanoids.

Preparation and Reaction of Stable β -Keto bis-sulfonium ylid. Y. Nakajima, M. Muroi, J. Oda, and Y. Inouye. *Agr. Biol. Chem.*, **37**, 277 (1973).—Novel carbonyl-stabilized bis-sulfonium ylids were synthesized for the purpose of revealing their physicochemical properties as well as exploiting their synthetic application. The treatment of these ylids with phenylisocyanate gave stable bis-carbamoyl sulfonium ylids. The reaction with some α,β -unsaturated carbonyl compounds resulted in the Michael type addition to afford the corresponding bis-cyclopropane derivatives. The solvent polarity dependence of stereochemistry of the cyclopropane formation was observed in the reaction of ylids with chalcone.

Studies on the Ortho-phosphoric Acid Method for the Pyrethrum Assay. N. Baba, M. Kirihata, M. Ohno, T. Takano, and K. Kono. *Botyu-Kagaku*, **37**, 155 (1972), in Japanese.—Coloration with ortho-phosphoric acid was tested on the synthetic pyrethroids, and pyrethrins I and II alone were found to be responsible for the pink-coloration, but not with jasmolins I and II. Practical application of this method for natural pyrethrum assay as tested with dried flowers of domestic Shirayuki strain and of the Kenya flower proved that a fine agreement was obtained between the analytical values by the conventional acidmetry and those by the present colorimetric estimation, provided that the relative content of six insecticidal components or the content of pyrethrins I and II relative to the total pyrethrins in the test flowers be equal to those of the standard. Otherwise, a suitable correction for the relative contents may improve the evaluation of total pyrethrins by the present colorimetric method.

Polymer Chemistry

Shear Creep Studies of Narrow-Distribution Poly (*cis*-isoprene). II. Extension to Low Molecular Weights. N. Nemoto, H. Odani, and M. Kurata. *Macromolecules*, **5**, 531 (1972).—Shear creep measurements have been made on six poly (*cis*-isoprene) samples of narrow molecular weight distribution with the molecular weights ranging from 3100 to 43,000. The viscosity η , the steady-state compliance

J_e , and the maximum relaxation time τ_m are calculated from the creep curves. The critical molecular weight M_e at which the logarithmic plot of η against M exhibits an abrupt change in slope from 1.0 to 3.7 is found to be about 10,000. The molecular weight dependence of J_e also undergoes a rapid change near $M_b=50,000$. At low molecular weights, J_e is approximately linearly dependent on M , in agreement with the prediction of the Rouse theory, while at high molecular weights, it is nearly independent of M . The maximum relaxation time τ_m varies as the 3.7 power of M over a wide range of molecular weight, from 6000 to 1,120,000. The entanglement compliance J_{eN} is found to be about 1.6×10^{-7} cm²/dyn for samples having $M > M_b$, which is merely one-eighth to one-tenth of J_e . The average molecular weight M_e between entanglement coupling points is about 3000, as evaluated from J_{eN} .

Creep Behavior of Polymer Solutions. III. Creep Compliance of Concentrated Polystyrene Solutions. Y. Einaga, K. Osaki, M. Kurata, and M. Tamura. *Macromolecules*, **5**, 635 (1972).—The creep compliance $J(t)$ of polystyrene solutions in chlorinated biphenyl was measured at various temperatures (−20 to 30°C). The ranges of molecular weight M and concentration c were 9.7×10^4 – 1.8×10^6 and 10–60 g/dl, respectively. The temperature coefficient of the fractional free volume as evaluated from a_T , the shift factor obtained from the time-temperature reduction method, was approximately equal to that for undiluted polystyrene over the whole range of concentration investigated. The time-concentration reduction method was applied to the creep compliance in the transition region, giving the shift factor a_c which is proportional to the segmental friction coefficient. The viscosity divided by the segmental friction coefficient was proportional to the 3.4th power of the product cM . The time-concentration reduction method was not applicable to the relaxation modulus calculated from $J(t)$ in the flow and plateau regions. This result indicates that the strength of one or a few relaxation mechanisms at the longest time end are proportional to the third or a higher power of c , in contrast to that in the plateau region which was found to be proportional to c^2 .

Shear Creep Studies of Narrow-Distribution Poly(*cis*-isoprene) III. Concentrated Solutions. N. Nemoto, T. Ogawa, H. Odani, and M. Kurata. *Macromolecules*, **5**, 641 (1972).—In order to elucidate the behavior of the steady-state compliance J_e as function of polymer concentration, shear creep measurements were made on concentrated solutions of narrow-distribution poly(*cis*-isoprene) with molecular weights M of 153,000 and 395,000 in chlorinated biphenyl, and also in a poly(*cis*-isoprene) of molecular weight 3100 as a solvent. In all the solutions studied, J_e is found to exhibit a rather complicated dependence on polymer concentration c . At high concentrations, J_e is independent of M and is proportional to c^{-3} . With decreasing c , J_e reaches to a maximum, then passes through a small minimum, and increases again. In the last region of c , J_e is approximately proportional to $c^{-1.5}$ and to M . The maximum and minimum in J_e are shifted toward lower values of c as the molecular weight is increased, but are not affected by the nature of solvent. In contrast to these properties of J_e , the pseudoequilibrium compliance J_{eN} decreases monotonously with increasing concentration as $J_{eN} \propto 1/c^2$, showing no complexity over the wide range of c from about 10 wt% to the undiluted state. The viscosity η_c and

the maximum relaxation time τ_{mc} at constant friction factor also varied monotonously as functions of c .

Randomly Branched Polymers. I. Hydrodynamic Properties. M. Kurata, M. Abe, M. Iwama, and M. Matsushima. *Polymer J.*, **3**, 729 (1972).—A sample of copolymer of styrene and 1,4-divinyl-2,3,5,6-tetrachlorobenzene was prepared and fractionated. Using the fractionated copolymers, effects of chain branching on the intrinsic viscosity and sedimentation coefficient were studied experimentally. It was found that in both theta and good solvents, the intrinsic viscosity of the branched polymers obeyed a new semiempirical relationship, $[\eta]_b = g^{0.6}[\eta]_l$. Here $[\eta]_l$ is the intrinsic viscosity of a linear polymer having the same molecular weight as the branched one and g is the contraction factor which is defined as the ratio of the mean-square radii of gyration between the branched and the linear polymers, *i.e.*, $g = \langle S^2 \rangle_b / \langle S^2 \rangle_l$. It was also found that the sedimentation coefficient in theta solvent agreed with the theoretical value obtained by Kurata and Fukatsu. The degree of branching estimated from the intrinsic viscosity or sedimentation coefficient was in close agreement with the value estimated from consideration of copolymerization kinetics.

Randomly Branched Polymers. II. Computer Analysis of Gel-Permeation Chromatogram. M. Kurata, H. Okamoto, M. Iwama, M. Abe, and T. Homma. *Polymer J.*, **3**, 739 (1972).—An iterative computer method was proposed for estimating the degree of branching and molecular weight distribution simultaneously from a pair of measurements on intrinsic viscosity and gel-permeation chromatography. The validity of the method as applied to randomly branched polymers was tested by using both fractionated and unfractionated samples of branched polystyrenes. It was experimentally concluded that the average number of branch points per unit molecular weight, λ , can be determined by this method with accuracy of about 15%, and the weight-average molecular weight with accuracy of about 10%.

Infinite-Dilution Viscoelastic Properties of Star Polystyrene with Nine Arms. Y. Mitsuda, K. Osaki, J. L. Schrag, and J. D. Ferry. *Polymer J.*, **4**, 24 (1973).—The storage and loss shear moduli, G' and G'' , have been measured for solutions of star polystyrene with average number of arms 8.7 and weight-average molecular weight 5000000, by use of the Birnboim-Schrag multiple-lumped resonator. The frequency range was 106 to 6060 Hz and the concentration range 0.001 to 0.013 g/ml. Decalin and di-2-ethyl hexyl phthalate were used as solvents at their respective Θ -temperatures, 15 and 21°C, and α -chloronaphthalene as a good solvent at 25°C. The extrapolated intrinsic moduli agree well with the predictions of the Zimm-Kilb theory as evaluated by Osaki and Schrag if the hydrodynamic interaction parameter h is taken as 0.40 in the Θ -solvents and 0.25 in α -chloronaphthalene. The product $h \alpha_\eta$, where α_η is the expansion factor of the excluded volume effect as evaluated from the intrinsic viscosity, is about 0.40 instead of 0.21 as observed for linear polymers. The origin of this unexpectedly large value is unclear.

Flow Properties of Copolymer Solutions. Measurements with a Cone- and Plate Viscometer. N. Nemoto, K. Okawa, and H. Odani. *Bull. Inst. Chem.*

Res., Kyoto Univ., **51**, 118 (1973).—A cone-and-plate viscometer is constructed, which is suitable for measurements of viscosities from 1.0×10^{-1} to 1.0×10^7 poises at rates of shear of 3.60×10^{-2} to $1.41 \times 10^2 \text{ sec}^{-1}$.

Some results are given of measurements on solutions of three different types of copolymer, *i.e.* the block, the alternating, and the random copolymers, of methyl methacrylate (MMA) and styrene (S) with nearly equimolar composition. In chlorinated biphenyl, a good solvent for the both components, all the solutions exhibited the non-Newtonian flow behavior. The shear rate-temperature superposition was achieved for viscosity data of solutions of the alternating and the random copolymers but not for the solution of triblock copolymer consisted of linear chains of PMMA-PS-PMMA. In a mixture of diethyl phthalate and dioctyl phthalate, in 3 : 7 mole ratio, the viscosity of the solution depended on shear history as well as shear rate.

Studies on the Structure of Filamentous Bacteriophage fd. I. Physicochemical Properties of Phage fd and its Components. K. Ikehara, Y. Obata, H. Utiyama, and M. Kurata. *Bull. Inst. Chem. Res., Kyoto Univ.*, **51**, 140 (1973).—Detailed structural information of phage fd has been obtained by using physicochemical techniques. Spectrophotometric results indicate that the DNA in the virion exhibits a hypochromicity about 60% as large as that of double-stranded native DNA, and the major native coat protein contains about 90% α -helical conformation. From the electrophoretic mobility of the phage protein in SDS polyacrylamide gel, it was elucidated that the A-protein, which is considered to bind with the tip of the virion, exists as an aggregate consisting of four molecules. The molecular weights of the various constituents of the virus were determined as: DNA, 1.85×10^6 daltons; A-protein, 7.4×10^4 daltons; A-protein aggregate, 30×10^4 daltons; B-proteins, smaller than 1×10^4 daltons.

Rheology—Polymer Solutions. K. Osaki. *Kobunshi-Kagaku no Tenbo (Annual Review of Polymer Science)*, **3**, 184 (1973), in Japanese.—A review article of recent studies on rheological properties of polymer solutions and melts. The subjects covered are:

1). Viscoelastic properties of concentrates of linear and branched polymers. The effect of varying molecular weight distribution was discussed with regard to linear polymers. Rheological properties of three types of branched polymers, *i.e.*, star-shaped, comb-shaped, and randomly (statistically) branched polymers, were reviewed,

2). Viscoelastic properties of polymers at infinite dilution. Intrinsic complex moduli were reviewed for a wide variety of polymer-solvent combinations including branched polymers. Hydrodynamic theories for dilute polymer solutions appeared in 1972 were introduced.

3). Viscoelastic properties of dilute polymer solutions at very high frequencies. Experimental results for dynamic viscosity of dilute polymer solutions at very high frequencies were collected. It was shown that at least two relaxation regions of different relaxation mechanisms exist in dilute polystyrene solutions. Current theories were assessed on the basis of experimental results.

Polymer Solutions. M. Kurata. *Kobunshi-Kagaku no Tenbo (Annual Review of Polymer Science)*, **3**, 193 (1973), in Japanese.—A review article of recent studies on

physico-chemical properties of polymer solutions. The subjects covered are:

- 1). Effect of molecular weight distribution on the phase equilibrium, with emphasis of the role of light scattering measurements as a tool for precise determination of phase diagram.
- 2). Analysis of the composition distribution in copolymer chains by means of the cross fractionation, the sedimentation equilibrium and the thin layer chromatography.
- 3). Gel permeation chromatography. Its principle and application to randomly branched polymers.
- 4). Hydrodynamic properties of branched polymers.
- 5). Conformational statistics of linear chain molecules. Monte Carlo calculations of the average shape of molecules and the excluded volume effect.
- 6). Theories of hydrodynamic properties of polymer chains.
- 7). Statistical theory of semi-flexible chains.
- 8). Light scattering. Theoretical and experimental studies of the particle scattering factor from linear chain molecules and the quasi-elastic Raileigh scattering.

Numerical Calculations of the Viscoelastic Properties of Solutions of Branched Polymers Based on the Zimm-Kilb Theory. K. Osaki and J. L. Schrag. *J. Polymer Sci. Part A2*, **11**, 549 (1973).—Numerical calculations were performed for the viscoelastic properties of dilute solutions of branched star polymers with equal branch lengths as formulated in terms of a bead-spring model by Zimm and Kilb without using the integrodifferential equation approximation method to calculate the eigenvalues. The complex modulus and complex viscosity were calculated as functions of frequency for various combinations of the number of branches f (4, 8, and 13), the number of beads in one branch N_b ($=N/f$; 20 to 100, where $N+1$ is the total number of beads, N the number of springs in the molecule) and the reduced hydrodynamic interaction parameter h ($=h/N^{1/2}$; 0.05 to 0.3, where h is the hydrodynamic interaction parameter of Zimm and Kilb). Characteristic quantities related to intrinsic viscosity and steady-state compliance were tabulated. Non-free draining behaviors of viscoelastic quantities were predicted when $h=0.25$ and draining effect became remarkable as h decreased. For h values larger than 0.25 was predicted a "super-non-free-draining" behavior which was not expected from the approximation method based on integrodifferential equation.

Flexibility of Tropocollagen from Sedimentation and Viscosity. H. Utiyama, K. Sakato, K. Ikehara, T. Setsuiye, and M. Kurata. *Biopolymers*, **12**, 53 (1973).—Sedimentation constant and intrinsic viscosity were measured on purified tropocollagens extracted from earthworm-cuticle and lathyritic ratskin. A Cartesian diver viscometer was used to make viscosity measurements at small shear stress and to avoid the effects of surface forces. By comparing the experimental data with the hydrodynamic theories of wormlike-coil of Ullman a value of 1300Å has been assigned for the persistence length of these tropocollagens. Other factors which may affect the estimate are discussed.

Construction and Use of Rotating Cylinder Viscometers. N Sugi, Y. Tsunashima, K. Ikehara, and H. Utiyama. *Japan. J. Appl. Phys.*, **11**, 1547 (1972).

—Three types of simplified rotating cylinder viscometers for dilute macromolecular solutions, two for dilute aqueous solutions, and the third for non-aqueous solutions, have been constructed, and their use are described in detail. An eddy-current drive with a permanent magnet rotated by a geared synchronous motor has been utilized in the viscometers yielding a very low shear stress in the range of $10^{-4}\sim 10^{-2}$ dynes/cm². The intrinsic viscosity extrapolated to zero shear stress could be measured within the experimental error of $\pm 1\%$. Applications of the viscometers to studies of organic solutions of a poly- α -methylstyrene sample with molecular weight of 6.85×10^6 , and of aqueous solutions of tropocollagen extracted from earthworm cuticle are also presented

Thermodynamic and Conformational Properties of Styrene—Methyl Methacrylate Block Copolymers in Dilute Solution. VI. Chain Conformations Disclosed by Thin-Layer Chromatography. F. Kamiyama, H. Inagaki, and T. Kotaka. *Polymer J.*, **3**, 470 (1972).—The development characteristics in thin-layer chromatography was studied for block copolymers of BAB-type with equimolar composition but different molecular weights, where A and B are polystyrene (PS) and poly(methyl methacrylate) (PMMA), respectively. The values of R_f (rate of flow) obtained with a developer composed of nitroethane and acetone decreased with increasing molecular weight, whereas those with other developers, which behave as good solvents for both PS and PMMA, were little dependent on molecular weight. In view of our previous finding that the molecular weight dependence of R_f appears only when phase separation of sample polymer takes place during the development, the solution state of block copolymers in the solvent mixture of nitroethane and acetone was investigated by means of phase equilibrium and ultracentrifugation. No phase separation was observed. Thus a pertinent elucidation for the molecular weight dependence of R_f was given by taking into consideration that the random flight conformation of block copolymers collapses due to *intramolecular* phase separation between the block portions of PS and PMMA, which will be brought about because both solvents are nonsolvents for PS but good solvents for PMMA.

A Nuclear Magnetic Resonance Study on the Adsorption of Poly(methyl methacrylate) at a Solid/Liquid Interface. T. Miyamoto and H.-J. Cantow. *Makromol. Chem.*, **162**, 43 (1972).—The adsorption and desorption behavior of tactic poly(methylmethacrylate) (PMMA) chain on silica gel from chloroform solution are investigated by using high-resolution NMR spectroscopy.

The conformation of PMMA chains adsorbed on silica and the effects of polar additives on polymer adsorption are discussed.

It is shown that the adsorption of PMMA on silica surface is so strong as to restrict highly the polymeric motion of PMMA at segmental level. The conformation of PMMA adsorbed on silica gel surface is considered to be a uniformly adsorbed and relatively compressed form. The NMR technique is very effective to estimate the fraction of segments of which the segmental motion is restricted because of the adsorption on silica gel.

The methanol/silica interaction is stronger than the PMMA/silica interaction,

and methanol reduces rapidly PMMA adsorption on silica. The rate of adsorption displacement of PMMA by methanol is relatively rapid and PMMA almost reaches the equilibrium adsorption value within 30 min at room temperature.

Molecular Sieve Effects in Thin-Layer Chromatography. N. Donkai and H. Inagaki. *J. Chromatogr.*, **71**, 473 (1972).—A series of investigations was carried out to establish the experimental conditions under which fractionation by molecular size occurs due to molecular sieve effects in thin-layer chromatography with macroporous silica gels. Molecular sieve effects appear on chromatoplates pre-eluted with a developer before the sample development when adsorptive interactions between polymer and adsorbent are eliminated by choosing an appropriate solvent for the developer. It is pointed out that the phase ratio, defined as the weight of developer per unit weight of adsorbent, should be sufficiently high to induce molecular sieving. A quantitative discussion is given of the enhancement of the resolution with respect to molecular weight in the separation, compared with results obtained by gel permeation chromatography with the same silica gels.

Separation of Atactic and Syndiotactic Methyl Methacrylate Polymers by Thin-Layer Chromatography. H. Inagaki and F. Kamiyama. *Macromolecules*, **6**, 107 (1973).—Separation of atactic and syndiotactic methyl methacrylate polymers (PMMA) has been investigated with the thin-layer chromatographic technique (tlc). Mixtures of ethyl acetate (ETOAc) and isopropyl acetate (*i*-PrOAc) and of acetonitrile (MeCN) and methanol (MeOH) were found to be effective as developer. Values of R_f (normalized rate of flow of the polymeric species) obtained with the mixture (ETOAc+*i*-PrOAc) increased with decrease in both syndiotactic content (T_s) and molecular weight (M), whereas those with the mixture (MeCN+MeOH) increased with increase in T_s but with decrease in M . No solvent pair which allows the separation solely by the difference in T_s has been found. These development characteristics were discussed on the basis of separation mechanisms proposed previously. The R_f values determined with each mixture were expressed as a function of T_s and M . With the aid of the functions thus established, a procedure to estimate T_s of a given sample from values of R_f obtained by the use of both mixtures was described, and proved to be applicable. A PMMA sample, which has been artificially prepared so that it had appreciable heterogeneity in T_s as well as M , was chromatographed with the mixture (MeCN+MeOH), and into two components. Despite such success in the separation it is pointed out that the experimental procedure was too complicated to be applied generally to practical problems, this being indicative of the limitation of applicability of tlc to polymer fractionation.

The Properties of Transparent Film Made from Linear Polyethylene by Irradiation Cross-Linking. R. Kitamaru, H.-D. Chu, and S.-H. Hyon. *Macromolecules*, **6**, 337 (1973).—Highly transparent films were made from linear polyethylene by irradiation cross-linking. The thermodynamic properties as well as the crystalline structure of the films were studied. It was confirmed that the transparent films have very high melting temperatures and a highly ordered and stable crystalline phase, but a rather low degree of crystallinity. X-Ray studies revealed

that the samples have a very special spatial orientation of the crystalline phase. *C* axes are located almost perfectly parallel to the film plane, and crystal planes (110) and (200) are oriented preferentially parallel to that plane. The origin of the transparency is discussed with respect to this spatial orientation of the crystalline phase.

The Orientation of Crystal Planes in Polyethylene Crystallized under Compression. S.-H. Hyon, H. Taniuchi, and R. Kitamaru. *Bull. Inst. Chem. Res., Kyoto Univ.*, **51**, 91 (1973).—The orientation of the crystal planes (200) and (110) appearing in a lightly cross-linked polyethylene when its molten specimen is compressed between two metal plates are studied with three different X-ray techniques. It is confirmed that the (200)-orientation parallel to the film surface of the sample first appears at a relatively low degree of compression and the (110)-orientation follows at higher degrees of compression. These two kinds of orientation for the crystal planes were also observed for polyethylene samples through procedures involving two-dimensional stretching of molecular chains.

Simultaneous Estimation of Particle Size, Relative Refractive Index and Concentration of Latices by Turbidity Measurements. M. Hosono, S. Sugii, O. Kusudo, and W. Tsuji. *Bull. Inst. Chem. Res., Kyoto Univ.*, **51**, 104 (1973).—A method to estimate simultaneously the size and concentration of particles in latices and the relative refractive index of those to the surrounding medium by turbidity measurements at three different wave-lengths is proposed. The values obtained for polystyrene latex by this method agreed well with those obtained by other methods. The validity of this method is discussed.

Some Textile Properties of Acrylic Acid Grafted Polypropylene Fabric Treated with Metallic Salts under Various Conditions. T. Ikeda, M. Hamanaka, W. Tsuji, and Y. Ikeda. *Sen-i Gakkaishi*, **28**, 449 (1972), in Japanese.—The treatments of acrylic acid grafted polypropylene fabrics with metallic salts were examined in relation to the textile properties such as hygroscopic property and thermooxidative stability.

Carboxylic groups of the acrylic acid grafted polypropylene fabrics were converted to sodium salts with sodium carbonate or sodium acetate. Then, a portion of each treated fabrics was further treated with calcium acetate so that sodium carboxylates in the fabrics were altered to calcium salts.

It was found from the infrared absorption spectra and moisture regain of these four kinds of fabrics that the degree of conversion to the corresponding salt-forms and moisture regain are more increased by using sodium carbonate in the first step of the treatment than by using sodium acetate.

The thermooxidative stability of calcium and zinc salts of acrylic acid grafted polypropylene fabrics, which have already been reported to have better stability than the grafted fabrics untreated or treated with other inorganic metals, is also improved when sodium carbonate was used in the first step compared to the use of sodium acetate. These results are explained if the conversion of the carboxyl group in the fabrics to other salt-forms is considered.

When sodium carbonate was used in the first step, further attempts were made

to increase the conversion with increasing concentration of the metallic salt in the treating solutions as well as longer period of reaction time. As the result, it is suggested that the thermooxidative stabilities of the grafted fabrics in the forms of calcium or zinc salts are very sensitive to small changes of conversion even in a high degree of conversion, but the moisture regains of those, including sodium salt-form, are rather insensitive to them at a higher level.

It may be concluded from this study that in the chemical modification of fibers by the graft copolymerization with acid group containing monomers such as acrylic acid and aftertreatment with metallic salts, the degree of conversion of carboxylic groups in the grafted fibers to suitable metallic salt-forms are very important.

Thermo-Oxidative Stability of Acrylic Acid Grafted Nylon 6 Fabrics.

T. Ikeda, W. Tsuji, and Y. Ikeda. *Sen-i Gakkaishi*, **29**, 38 (1973), in Japanese.—The thermo-oxidative stability (*i.e.* the retention of warp tensile strength of fabric after heat exposure at 130°C for a long duration) of acrylic acid grafted nylon 6 fabrics, treated with some metallic salts or tris(1-aziridinyl)phosphine oxide (APO), was studied.

The results obtained were different in some aspects from those of polypropylene fabrics reported previously. The thermo-oxidative stability of nylon 6 fabric was improved to some extent by the grafting of acrylic acid. The conversion of carboxylic groups in the grafted nylon 6 fabrics to a metallic salt-form was carried out with aqueous solutions of metallic salts. When calcium, chromium or nickel salts were used, the metallization was more or less effective on the stability of fabrics, but the effects were not so remarkable as in the case of the grafted polypropylene. The stability in copper salt-form was deteriorated somewhat by heat, but the extent of the damage was not so significant as in the case of acrylic acid grafted polypropylene. The fact that the grafting and the subsequent chromium salt formation improve the stability of nylon 6 fabrics but rather spoil the stability of polypropylene may suggest that some differences are present between the mechanisms of thermo-oxidative degradation of the two polymers, although a similar radical mechanisms have been assumed. The treatment with APO, which imparted a better stability to acrylic acid grafted polypropylene fabrics, was also effective for ungrafted nylon 6 fabric but was not for the grafted nylon 6 fabrics, since the add-on of APO attained was small.

Thermal Analysis of Acrylic Acid Grafted Polypropylene Fabric. (I)

Differential Scanning Calorimetry. T. Ikeda, W. Tsuji, and Y. Ikeda. *Sen-i Gakkaishi*, **29**, 43 (1973), in Japanese.—Polypropylene (PP), acrylic acid grafted PP fabrics and those treated with aqueous solutions of some metallic salts or tris(1-aziridinyl)phosphine oxide (APO) were studied by differential scanning calorimetry (DSC).

DSC curves of all the samples show no oxidative exotherm in nitrogen atmosphere. On the other hand, acrylic acid grafted PP fabrics with percent grafting of more than 28% show a relatively large exotherm above 170°C in air, and this is shifted to lower temperatures compared with 250°C of original PP fabric, suggesting that PP fabric becomes susceptible to oxidative degradation by acrylic acid grafting. Large broad exotherms appear in air above 180°C in the DSC curves of acrylic acid grafted PP fabrics treated with metallic salts or APO even in sample with a lower percent grafting

(19.5%), which is different from those of grafted and untreated fabrics. The DSC curve of acrylic acid grafted and copper salt treated PP fabric shows two peaks successively in the vicinity of these exotherms which may be considered as the indication of copper ion catalyzed oxidative degradation of PP. These exothermic peaks in the DSC curves of the acrylic acid grafted and after-treated PP fabrics are not clearly assigned.

Heat of fusion of PP component in the acrylic acid grafted PP fabrics is lowered by the grafting, and a linear relationship is obtained when the heats of fusion of the samples with different percent of grafting are plotted against percent grafting.

Effect of Zinc Fluoroborate Catalyst on Thermooxidative Stability of Acrylic Acid Grafted Polypropylene Fabrics Treated with Tris(1-Aziridinyl) Phosphine Oxide. T. Ikeda, M. Hamanaka, W. Tsuji, and Y. Ikeda. *Sen-i Gakkaishi*, **29**, 70 (1973), in Japanese.—Effect of zinc fluoroborate ($\text{Zn}(\text{BF}_4)_2$) catalyst in the treatment of acrylic acid grafted polypropylene fabric with tris(1-aziridinyl) phosphine oxide (APO) was studied.

Weight increase (resin add-on) by APO-treatment and moisture regain of the polypropylene fabrics grafted with acrylic acid and further treated with dimethylformamide solution containing 5% APO are nearly equal regardless of the presence of $\text{Zn}(\text{BF}_4)_2$, while the weight increase of original ungrafted polypropylene fabric treated with APO and $\text{Zn}(\text{BF}_4)_2$ is higher than that of the sample treated without $\text{Zn}(\text{BF}_4)_2$. These facts suggest that the grafted acrylic acid chains have some catalytic action in this treatment and use of $\text{Zn}(\text{BF}_4)_2$ is not always necessary in the case of the grafted fabrics.

As $\text{Zn}(\text{BF}_4)_2$ has some deteriorative effect upon thermooxidative stability (measured by retention of warp tensile strength of the fabric after heat exposure at 100°C) of original polypropylene and the grafted polypropylene fabrics treated with APO— $\text{Zn}(\text{BF}_4)_2$ or $\text{Zn}(\text{BF}_4)_2$ alone, the elimination of use of $\text{Zn}(\text{BF}_4)_2$ catalyst in the treatment of the grafted fabrics with APO results in better thermooxidative stability of the fabrics and also some practical advantages, such as storage stability of the treating APO solution, etc.

Further experiments were made on the thermooxidative stability of the grafted polypropylene fabrics treated with phosphorus-containing compound (butyl acid phosphate-metal acetate system) or nitrogen-containing resins (methylol melamine and ethyleneurea), and no improving effects were observed with these treatments.

Light Resistance of Acrylic Acid Grafted Polypropylene or Nylon 6 Fabrics. T. Ikeda, M. Hamanaka, W. Tsuji, and Y. Ikeda. *Sen-i Gakkaishi*, **29**, 80 (1973), in Japanese.—Light resistance of polypropylene (PP) and nylon 6 fabrics, grafted with acrylic acid and then treated with aqueous solutions of some metallic salts or tris (1-aziridinyl)phosphine oxide (APO), was studied by evaluating the retention of warp tensile strength of the fabrics after exposure to xenon arc lamp or sunlight.

Larger loss in strength of original untreated PP fabric after exposure as a result of the extraction with benzene may be explained by the removal of included stabilizer by the extraction.

Grafting of acrylic acid onto PP fabric and further treatment with aqueous

solution of metallic salts cause unfavorable effect on light resistance due to the presence of carbonyl groups in the grafted side chains.

The most effective method to improve the light resistance of acrylic acid grafted PP fabrics is the after-treatment with APO. The higher the percent grafting or/and concentration of APO treating solution the better resistance is attained.

On nylon 6 fabric, nearly similar results to the case of PP fabric are obtained by grafting and treating with metallic salts, but the effect of APO is not clear with acrylic acid grafted nylon 6 fabrics as the add-on of APO is not so high as the case of acrylic acid grafted PP fabrics.

Some Aspects of Nonisothermal Crystallization of Polymers. I. Relationship Between Crystallization Temperature, Crystallinity, and Cooling Condition. K. Nakamura, T. Watanabe, K. Katayama, and T. Amano. *J. Appl. Polym. Sci.*, **16**, 1077 (1972).—The changes in temperature and crystallinity of polymers during nonisothermal crystallization were theoretically analyzed assuming a cooling condition under which heat transfer occurs at a rate proportional to the difference in temperature between polymer and the environment. When a plateau appears in the temperature change during crystallization, crystallization temperature can be predicted by a simple method. This method gives nearly the same value as that obtained by successive calculations of temperature and crystallinity throughout the whole process. In addition, a graphic method is presented to predict crystallization temperature. By using the plateau temperature observed in melt-spinning experiments, the crystallization rate under molecular orientation is evaluated. Furthermore, a method applicable to estimating the ultimate crystallinity is proposed. A rough estimation of the increase in the rate of crystallization under molecular orientation was carried out for very high-speed spinning of poly(ethylene terephthalate).

Some Aspects of Nonisothermal Crystallization of Polymers. II. Consideration of the Isokinetic Condition. K. Nakamura, K. Katayama, and T. Amano. *J. Appl. Polym. Sci.*, **17**, 1031 (1973).—The fundamental equation for an analysis of non-isothermal crystallization was written on the assumption of the isokinetic conditions in the following form:

$$X(t) = 1 - \exp \left[- \left(\int_0^t K(T) d\tau \right)^n \right]$$

where $X(t)$ is the degree of phase transformation at time t , and n is the Avrami index determined in the isothermal experiments, $K(T)$ is connected with the crystallization rate constant of the isothermal crystallization, $k(T)$, through the relation $K(T) = k(T)^{1/n}$. The equation is derived on the basis of the well-known theory of phase transformation. Experiments of nonisothermal crystallization of high-density polyethylene were carried out under various cooling conditions. The change in crystallinity during the process was followed by using the above equation in the course of the primary crystallization. A procedure of the analysis of the whole, including both the primary and secondary processes, is suggested as an eminently practical one on a more general assumption.

Biochemistry

Energy Calculations on Di- and Poly-L-Proline. K. Nishikawa and T. Ooi. *Bull. Inst. Chem. Res., Kyoto Univ.*, **50**, 94 (1972).—The problem of distortion of a pyrrolidine ring in a prolyl residue is treated in terms of the rotational angle ϕ about N-C α bond. Assuming that the C γ atom in the ring occupies one of the two representative positions, energy maps of poly-L-proline and di-peptide Pro-Gly can be calculated with the variables of ϕ , ψ and ω . Polyproline in the trans-planar configuration has two minima in the lower energy contour area involving polyproline II conformation, and in the cis-configuration has a single deep minimum. Two other areas of lower energies are found mainly in the (ω , ψ) maps under the constant values of ϕ . The energy maps of Pro-Gly resemble the usual dipeptide maps in the sterically allowable range of ϕ .

Molecules and Structure of Regular Molecular Assemblies. I. Ring Forming Ellipse. Y. Hiragi. *Bull. Inst. Chem. Res., Kyoto Univ.*, **50**, 584 (1972).—For the elucidation of the relation between characters of molecules such as shapes and positions of the bonding sites, and the structure of their regular assemblies, a ring composed of identical ellipse was investigated as the simplest case. It was shown that the radius of ring and the number of the constituent ellipse were dependent on the length of the major and minor axes, and position of the bonding site of the ellipse.

Thermally Induced Denaturation of Intramolecularly Cross-Linked Bovine RNase A. S. Takahashi and T. Ooi. *Bull. Inst. Chem. Res., Kyoto Univ.*, **51**, 153 (1973).—Thermally induced conformational denaturation of intramolecularly cross-linked RNase A (Lys⁷-Lys³⁷ or Lys³¹-Lys³⁷) was investigated to compare the non-modified protein. At pH 3.1, a transition temperature of 51° (RNase A, 46.5°) was obtained from difference spectra at 286 nm. Thermodynamic analysis of transition gave the following functions (the values for non-modified RNase A are in parentheses): $\Delta H^\circ=47$ (51), $\Delta F^\circ=2.32$ (1.91) in Kcal/mole, $\Delta S^\circ=145$ (160) e.u./mole, at 35°. The facts that ΔH° , ΔS° per residue in an ordered region seem to be remained constant irrespective of polypeptide species are commented.

Physical, Chemical and Morphological Studies of Spore Coat of *Bacillus subtilis*. Y. Hiragi. *J. Gen. Microbiol.*, **72**, 87 (1972).—Spore coat of *Bacillus subtilis* ATCC6051 was fractionated as described by Kondo & Foster (1967). X-ray diffraction, infra-red spectra, amino acid analyses and N-terminal amino acid studies showed that most of the fractions resembled each other in physical and chemical structure and constituents. Electron micrographs of sections and shadowed replicas of the coat fractions at various stages showed that the inner part of the coat disappeared during treatment; no drastic morphological change was observed throughout the fractionation.

The amounts of cystine in the coat and the coat fractions were less than in keratins. This result and solubilizing experiments suggested that the spore coat does not chemically resemble keratins.

Determination of Energy Parameters in Lennard-Jones Potentials from Second Virial Coefficients. M. Oobatake and T. Ooi. *Progress of Theoretical Physics.*, **48**, 2132 (1972).—The energy parameters in Lennard-Jones 6–12 potential between atoms (hydrogen, oxygen, nitrogen and carbon) were estimated from second virial coefficients of diatomic gases (H₂, O₂, N₂, NO and CO) and methane (CH₄), assuming the additivity of atomic potentials and the combination rules for unlike pairs. The results show that there is a certain relation between the two parameters (Van der Waals radius, r_w and the parameter of the attractive part, ϵ) when the calculated virial coefficients are in agreement with the experimental data over a wide range of temperature. Accordingly to the relation one can select reasonable sets of parameters for atoms, which reproduce the experimental virial coefficients. In general, the best fit values of r_w for H, N and C atom were somewhat greater than those usually adopted. As for H-H interaction the parameters obtained from the virial data of H₂ differ from those from CH₄ due presumably to deviation of simple additivity of atomic interactions. The relation between r_w and ϵ is available for justification or estimation of the energy parameters in atomic potentials, since any given atomic potential may have parameters which satisfy the relation or we can determine one of the parameters by the use of the relation if the other is found from the other measurements.

Conformational Properties of Poly(L-proline) Containing a Flexible Pyrrolidine Ring. W. L. Mattice, K. Nishikawa, and T. Ooi. *Macromolecules*, **6**, 443 (1973).—Two conformational maps for the dipeptide unit in the interior of poly-(L-proline) containing peptide bonds in the planar trans conformation are found to correctly predict the characteristic ratios experimentally observed for this polypeptide at 5 and 30°. These two conformational maps differ from previous maps in allowing for flexibility in the pyrrolidine ring. The maps are also consistent with Torchia's analysis of the ring vicinal coupling in the 220-MHz nmr spectrum of poly(L-proline) in aqueous solution.

A Reexamination of Electronic Effects in Ring-Substituted Phenyl Esters. Correlation of Spectral and Kinetic Properties with σ° . L. S. Cohen and S. Takahashi. *J. Amer. Chem. Soc.*, **95**, 443 (1973).—On the basis of UV spectroscopy, phenyl esters and lactones are considered to be devoid of "through resonance" between the aryl-oxygen atom and the para substituent. The true cause is the thermodynamic preference by the oxygen atom to overlap with the ester carbonyl rather than with the benzene ring. In support of this argument, the infrared carbonyl-stretching frequencies for 48 mono and polysubstituted phenyl hydrocinnamates are shown to correlate ($r=0.9997$) with σ° (or $\sum\sigma^\circ$) for the ring substituents, including a number of ortho substituents. Values of σ° for hydroxylic media have been reevaluated on the basis of 24 sets of data for systems in which resonance coupling of the reaction site with the benzene ring is improbable. Values of σ° (for nonpolar media) are derived by calculation: $\sigma_o^\circ(R) = \sigma_p^\circ(R) + 0.39\sigma^\circ(RCH_2)$. These σ° values are, in turn, used to correlate 33 sets of data on the intermolecular reactions of phenyl esters with various nucleophiles. The excellent correlations obtained serve to demonstrate that σ° is the appropriate parameter to be used in such correlations. Intramolecular reactions of phenyl esters, on the other hand, show a better correlation with σ^- .

It is tentatively considered that formation of a tetrahedral intermediate is rate limiting in intermolecular reactions of phenyl esters with nucleophiles, but that breakdown of tetrahedral intermediate is rate limiting in untramolecular cases.

Purification and Crystallization of Bacterial Leucine Dehydrogenase.

K. Soda, H. Misono, T. Shirako, K. Mori, and M. Sato. *Amino Acid and Nucleic Acid*, **27**, 84 (1973), in Japanese.—The distribution of leucine dehydrogenase in bacterial strains, and the preparation of crystalline enzyme from the cell-free extract of *Bacillus sphaericus* IFO 3525 are described. The high activity of enzyme was found in most strains of bacilli, and *Bacillus sphaericus* IFO 3525 was demonstrated to have the highest specific and total activity.

Leucine dehydrogenase was purified from the cell-free extracts to homogeneity and crystallized by addition of ammonium sulfate. The enzyme is homogeneous by criteria of ultracentrifugation and disc gel electrophoresis. The molecular weight is approximately 260,000 ($S_{20}^{\circ, w}$: 9.0S).

The enzyme catalyzes the oxidative deamination of L-leucine, L-valine, L-isoleucine, L-norvaline, while none of D-leucine, D-valine, L-alanine, L-glutamate and ϵ -aminocaproate is deaminated. The reductive amination of α -ketoisovalerate, α -ketoisocaproate, α -ketovalerate, α -ketocaproate and α -ketobutyrate are also catalyzed in the presence of NADH, ammonia and enzyme. NAD and NADH serve as the exclusive hydrogen acceptor and the donor, respectively.

Antitumor Activities of Bacterial Leucine Dehydrogenase and Glutaminase A.

T. Oki, M. Shirai, M. Ohshima, T. Yamamoto, and K. Soda. *FEBS Letters*, **33**, 286 (1973).—Antitumor activities of seven bacterial crystalline enzymes and one mammalian enzyme were investigated with Ehrlich ascites carcinoma *in vivo*. Among them leucine dehydrogenase of *Bacillus sphaericus* IFO 3525, and glutaminase A of *Pseudomonas aeruginosa* IFO 3080 were shown to be highly inhibitory to Ehrlich ascites carcinoma. Tumor-bearing mice treated with these enzymes showed a progressive increase in life span with increasing doses of the enzymes, *e.g.*, the dosage of 4 mg/kg \times 10 to 14 days produced 236 to 300% increase in mean survival time over controls. Alanine dehydrogenase and D-amino acids aminotransferase of *Bacillus sphaericus* IFO 3525, glutaminase B of *Pseudomonas aeruginosa* IFO 3080, amino acid racemase with low substrate specificity of *Pseudomonas striata*, lysine- α -ketoglutarate ϵ -aminotransferase of *Achromobacter liquidum* IFO 3084, and glutamate dehydrogenase of bovine liver were demonstrated to have substantially no antineoplastic activity.

Spectrophotometric Determination of Glyoxylic Acid with *o*-Aminobenzaldehyde and Glycine, and Its Application to Enzyme Assay.

K. Soda, S. Toyama, H. Misono, T. Hirasawa, and K. Asada. *Agr. Biol. Chem.*, **37**, 1393 (1973).—Glyoxylic acid reacted with *o*-aminobenzaldehyde and glycine to yield a yellow product, whose absorption maximum was at 440 m μ . Glycine could be replaced by ω -amino acids, *e.g.*, γ -aminobutyrate, and aliphatic amines, but not by α -amino acids. The effects of pH, kind and concentration of buffers, concentration of *o*-aminobenzaldehyde, and incubation time on the reaction were investigated to establish the optimum conditions. Microamounts of glyoxylate (0.05–1.5 μ moles) were

determined rapidly by this simple method with satisfactory results. α -Keto acids such as α -ketoglutarate reached far less effectively; almost no appreciable interference with quantitative estimation of glyoxylate occurred with them. This procedure is applicable for the assay of enzymes which catalyze the formation of glyoxylate, *e.g.*, isocitrate lyase and glycollate oxidase.

Purification, Crystallization, and Characterization of Glutaminases A and B from *Pseudomonas Aeruginosa*. K. Soda, M. Ohshima, and T. Yamamoto. *Proc. IV IFS: Ferment. Technol. Today*, 339 (1973).—Evidence was obtained for the occurrence of two isozymes of glutaminase in an extract of *Pseudomonas aeruginosa*. One of them, glutaminase A, is not adsorbed by DEAE-cellulose under the conditions employed, but glutaminase B is eluted with 0.01 M potassium phosphate buffer, pH 7.2, containing 0.03 M NaCl. Both the enzymes have been purified to homogeneity and glutaminase A has been crystallized. The molecular weights of glutaminases A and B are approximately 137,000 and 67,000, respectively. The K_m values were determined as follows, when the hydrolytic activity was assayed. Glutaminase A: L-glutamine (1.2×10^{-4} M), D-glutamine (8.5×10^{-4} M), L-asparagine (7.4×10^{-5} M), and D-asparagine (1.1×10^{-4} M). Glutaminase B: L-glutamine (1.8×10^{-4} M) and D-glutamine (2.3×10^{-4} M). Glutaminase A catalyzes the hydrolysis and the hydroxylaminolysis of L-glutamine, D-glutamine, L-asparagine, and D-asparagine. The hydrolysis of L-glutamine, D-glutamine, L-theanine, and D-theanine, and also the formation of the hydroxamates from these γ -glutamyl derivatives are catalyzed by glutaminase B, while both the enantiomers of asparagine are inert. L- γ -Glutamyl-P-nitroanilide is also hydrolyzed by isozyme B. Glutaminase A has an antineoplastic activity against Ehrlich ascites carcinoma, while glutaminase B shows little antitumour effect.

Cleavage Site Specificity of an Endonuclease from *Haemophilus influenzae* Strain H I. M. Takanami and H. Kojo. *FEBS Letters*, 29, 267 (1973).—In order to obtain unique fragments from phage fd replicative form DNA, attempts were made to search for a new endonuclease with cleavage site specificity. Among a variety of bacterial strains examined, a *Haemophilus* strain isolated at Research Institute for Microbial Diseases, Osaka University, was found to contain an endonuclease which split fd DNA at three different sites. This enzyme was successfully purified by collecting a fraction that preferentially destroyed the infectivity of double-stranded fd DNA upon transfection of single and double-stranded fd DNA into lysozyme-spheroplasts.

Specific Cleavage of Coliphage fd DNA by Five Different Restriction Endonucleases from *Haemophilus* Genus. M. Takanami. *FEBS Letters*, 34, 318 (1973).—Five species of restriction endonuclease from *Haemophilus* strains, including endonuclease R (Smith and Wilcox, 1970), endonuclease Z (Middleton *et al.*, 1972) and three new enzymes isolated in our laboratory, were purified, and their action on phage fd replicative form DNA was examined. Respective enzymes introduced duplex cleavages at different sites. Number of cleavage sites increased additively by the combination of enzymes with different cleavage site specificities. After isolating

a particular fragment from a digest, the fragment was further cleaved into smaller pieces by other enzymes. With these enzymes, it has become possible to derive a physical map of functional sites on fd DNA and to isolate DNA segments which are short enough for the determination of nucleotide sequences.

Physical Mapping of Transcribing Regions on Coliphage fd DNA by the Use of Restriction Endonucleases. M. Takanami and T. Okamoto. *Control of Transcription* (Plenum Publishing Co., New York, Ed. A. Hollaender), Chap. 12, 145 (1973).—Phage fd replicative form DNA was cleaved by *Heamophilus* restriction endonucleases, and the template activity of the resulting unique fragments and the size of synthesized products were compared with those on intact fd DNA. As a result, we could map the sites at which initiation and termination of transcription took place on fd DNA.

The Starting Nucleotide Sequences and Size of RNA Transcribed *in vitro* on Bacteriophage T3 DNA. T. Takeya and H. Fujisawa. *Biochim. Biophys. Acta*, **324**, 110 (1973).—RNA transcribed *in vitro* on phage T3 DNA by *Escherichia coli* and T3 RNA polymerases was characterized by means of the technique which labels the starting termini of RNA.

E. coli RNA polymerase predominantly initiated RNA synthesis with two different starting sequences: pppA-U-G- and pppG-U-. On synthesizing RNA at high salt concentration (0.15 M KCl), the sizes of both RNA species were about 37s, and at low salt concentration (0.03 M KCl), these chains grew to about 65S, corresponding to the size of the entire genome. The synthesized RNA predominantly hybridized to the r-strand of the template. It was, therefore, concluded that these two RNA chains were initiated at closely spaced sites near the left end of T3 DNA and terminated at either the site(s) about 25% of the distance along the starting end or the other end of the template depending on the salt concentration.

T3 RNA polymerase initiated RNA synthesis at least at four different sites, as the following four different termini were identified in the synthesized RNA: pppG-(R-)2-Yp, ppG-(R-)4-Yp, pppG-(R-)5-Yp and pppG-(R-)6-Yp. The size of the synthesized RNA was very heterogeneous, compared with these formed by host RNA polymerase.